Molecular Mechanisms of the Functional Coupling of the Helicase (gp41) and Polymerase (gp43) of Bacteriophage T4 within the DNA Replication Fork†

Emmanuelle Delagoutte and Peter H. von Hippel*

Institute of Molecular Biology and Department of Chemistry, University of Oregon, Eugene, Oregon 97403

Received June 7, 2000; Revised Manuscript Received January 10, 2001

ABSTRACT: Processive strand-displacement DNA synthesis with the T4 replication system requires functional "coupling" between the DNA polymerase (gp43) and the helicase (gp41). To define the physical basis of this functional coupling, we have used analytical ultracentrifugation to show that gp43 is a monomeric species at physiological protein concentrations and that gp41 and gp43 do not physically interact in the absence of DNA, suggesting that the functional coupling between gp41 and gp43 depends significantly on interactions modulated by the replication fork DNA. Results from strand-displacement DNA synthesis show that a minimal gp41−gp43 replication complex can perform strand-displacement synthesis at ∼90 nts/s in a solution containing poly(ethylene glycol) to drive helicase loading. In contrast, neither the Klenow fragment of *Escherichia coli* DNA polymerase I nor the T7 DNA polymerase, both of which are nonprocessive polymerases, can carry out strand-displacement DNA synthesis with gp41, suggesting that the functional helicase−polymerase coupling may require the homologous system. However, we show that a heterologous helicase−polymerase pair can work if the polymerase is processive. Strand-displacement DNA synthesis using the gp41 helicase with the T4 DNA polymerase holoenzyme or the phage T7 DNA polymerase−thioredoxin complex, both of which are processive, proceeds at the rate of ∼250 nts/s. However, replication fork assembly is less efficient with the heterologous helicase−polymerase pair. Therefore, a processive (homologous or heterologous) "trailing" DNA polymerase is sufficient to improve gp41 processivity and unwinding activity in the elongation stage of the helicase reaction, and specific T4 helicase−polymerase coupling becomes significant only in the assembly (or initiation) stage.

The ability to synthesize DNA rapidly and accurately is of central importance to all living organisms. To fulfill this function, most template-dependent replication polymerases carry both a 5′ → 3′ synthesis and a 3′ → 5′ editing activity. In addition, to achieve the overall rates of synthesis required by the cell cycle in each organism, these polymerases must function processively in both synthesis and editing of the nascent DNA, meaning that the polymerases must incorporate (and edit) many nucleotides within the elongating DNA chain per polymerase binding event. Such processivity is achieved in transcription by making the elongation complex very stable (for a recent review see ref *1*). However, this strategy is less useful in achieving processive synthesis in DNA replication because this synthesis must be terminated periodically to permit Okazaki fragment formation on the lagging strand. The more flexible processivity control required in DNA replication is achieved by means of a ring-shaped "processivity clamp" that encircles the double-stranded DNA. This clamp is loaded onto the DNA by an ATP-driven clamp loading complex, and then binds to the DNA polymerase to stabilize the latter on the template. Whereas the DNA polymerase on the leading strand, once clamped by its processivity factor, carries out uninterrupted DNA synthesis, the DNA polymerase on the lagging strand must dissociate from the clamp upon completion of each Okazaki fragment and then reassociate with a new clamp at the primer−template junction to initiate synthesis of the next fragment (*2*, *3*).

The machinery of DNA replication has other protein components that are charged with additional activities crucial to successful replication. These components include: (i) a primase to synthesize small RNA primers that are then elongated into Okazaki fragments by the DNA polymerase in lagging strand synthesis; (ii) a helicase to "open" the double-stranded DNA ahead of the fork to expose the single-stranded DNA templates and also to coordinate leading and lagging strand DNA synthesis through interactions with the primase; and (iii) a single-stranded DNA binding protein to bind cooperatively to (and protect) the transiently exposed single-stranded DNA, to hold open the replication fork, and to participate in the general regulation of the polymerase−primase−helicase complex (for a review see ref *4*). Two of these proteins, the processivity clamp of the DNA polymerase holoenzyme and the DNA helicase, are toroidal in shape. This enables them to encircle the DNA (double-stranded for the processivity clamp and single-stranded for the helicase) to form a topological link between the enzyme and the DNA (for a review on toroidal proteins see ref *5*).

The DNA replication machinery of bacteriophage T4, which is entirely encoded by the phage itself, requires only seven proteins to catalyze coordinated leading and lagging

† This work was supported in part by U. S. Public Health Service Research Grants GM15792 and GM29158. P.H.v.H. is an American Cancer Society Research Professor of Chemistry.

* To whom correspondence should be addressed. E-mail: petevh@molbio.uoregon.edu.

10.1021/bi001306l CCC: $20.00
Published on Web 03/10/2001

strand synthesis in vitro with a speed, processivity, and fidelity similar to those measured in vivo (for reviews see refs *6* and *7*). The DNA polymerase of the T4-coded replication complex is gp43.[1] In common with most other DNA polymerases, the gp43 core enzyme in isolation functions quite nonprocessively in incorporating nucleotide residues into the nascent DNA at physiological salt concentrations. It gains the processivity required for genome replication by interacting with the gp45 sliding clamp, which assembles cooperatively from monomers to form a ring-shaped trimeric complex of appropriate size to fit loosely around double-stranded DNA (*8*). Gp45 and the clamp loading machinery (gp44/62) constitute the T4-coded polymerase accessory proteins. The gp45 clamp is loaded onto the DNA at a primer−template junction by the gp44/62 complex in an ATP-dependent fashion, and multiple conformational changes occur in gp45 during the loading process (for a review see ref *9* and references within).

The gp41 helicase (*10*, *11*) is an A/GTPase (*12*) and forms a hexamer upon activation by A/GTP binding (*13*). This hexamer, which comprises the functional form of the gp41 helicase can, in isolation, use its single-stranded DNA-stimulated A/GTPase activity to translocate along single-stranded DNA templates with a 5′ → 3′ polarity and moderate processivity (*10*−*12*, *14*). Within the replication complex, the hexameric helicase unwinds the double-stranded DNA downstream of the fork, probably [by analogy to the helicase of bacteriophage T7 (*15*)] by working as a ring that encircles the lagging DNA template strand and binds to the leading template strand (*11*). The monomeric gp61 primase interacts with the hexameric gp41 helicase at the fork, producing RNA pentamers of specific sequence that prime the synthesis of Okazaki fragments on the lagging strand template (*16*−*20*). This specific gp41−gp61 interaction guarantees that RNA primers are synthesized at the fork and are properly placed within the moving replication fork, as required in discontinuous lagging strand DNA synthesis. The weak binary gp61−gp41 interactions, and the more stable ternary primosome complex formed from primase, helicase, and single-stranded DNA, have been well characterized (*21*, *22*). Numerous conformational changes of the primase are associated with binding to the helicase and to the single-stranded DNA of the replication fork (*22*).

The seventh member of the bacteriophage T4 replication machinery is gp32, the single-stranded DNA binding protein. It binds cooperatively to single-stranded DNA (*23*) and removes secondary DNA structures that might inhibit DNA synthesis, leading to a stimulation of the gp43 DNA polymerase activity (*24*). In the context of the replication fork, gp32 binds to the single-stranded DNA lagging strand generated behind the helicase at the moving replication fork and holds the fork open. This protein is also essential for confining RNA synthesis to sites used to start an Okazaki fragment, thus avoiding the synthesis of excess replication primers (*25*).

It is important to realize that two among these seven components, the leading strand DNA polymerase and the single-stranded DNA binding protein in lagging strand synthesis, can also serve as reporters ("spies") to monitor helicase activity in vitro by trapping the single-stranded DNA that is generated by the moving DNA helicase. As we report in this paper, the "spying" or "trailing" activity of the DNA polymerase serves to improve the processivity of the translocation and double-stranded DNA unwinding activities of the gp41 helicase at the replication, in the context of the replication elongation process.

A functional interaction between the T4 helicase and the DNA polymerase holoenzyme (including, at least, gp43, gp45, and gp44/62) was reported by Cha and Alberts (*26*), who showed that only the gp41 helicase seemed to be required for strand-displacement DNA synthesis by the DNA polymerase holoenzyme. They showed that the gp61 primase can be omitted without any effect on the strand-displacement replication rate and that the role of gp32 in this context is only to increase the number of replication forks but not to affect the rate of strand-displacement DNA synthesis. Subsequently, Spacciapoli and Nossal (*27*) characterized a T4 DNA polymerase mutant, A737V, that requires gp59 (the T4 helicase assembly or "loading" protein) to permit function of the mutant DNA polymerase within the T4 replication machinery to achieve effective strand-displacement DNA synthesis in the presence of gp41. These workers hypothesized that the DNA polymerase and the helicase do not operate separately and that an interaction between the gp41 helicase and the polymerase holoenzyme is required to permit the helicase and the entire replication complex to function efficiently at the replication fork. They suggested that this interaction is weaker with the mutant DNA polymerase and that strand-displacement DNA synthesis with the mutant DNA polymerase-containing holoenzyme required repeated reloading of the gp41 helicase onto the fork, thus accounting for the ongoing requirement for gp59.

Subsequently, Schrock and Alberts (*28*) measured the processivity and half-life of gp41 in the context of a complete in vitro DNA replication system (including gp41, gp43, gp44/62, gp45, gp32, and gp59). They suggested that gp41 must interact with the DNA polymerase holoenzyme at the replication fork, stabilizing the other protein components of the complex and being reciprocally stabilized in return. Finally, Dong et al. (*29*) reported that strand-displacement DNA synthesis at a primed DNA replication fork construct could be driven by gp41 and gp43 alone (in the absence of the other components of the DNA polymerase holoenzyme and using the macromolecular crowding agent poly(ethylene glycol) to drive helicase loading onto the fork), suggesting that the crucial functional interaction within the moving DNA replication fork was likely to be between the helicase and the DNA polymerase itself.

Building on these results we report here studies that attempt to define the physical nature and magnitude of these interactions between the T4 helicase and polymerase. We use the term "functional coupling" in these systems to

[1] Abbreviations: gp (number), gene product (number); ATPγS, adenosine 5′-3-*O*-(thio)triphosphate; ATP, adenosine 5′-triphosphate; GTP, guanosine 5′-triphosphate; γ^{32}P-ATP, γ^{32}P-adenosine 5′-triphosphate; dAMP, deoxyadenosine 5′-monophosphate; dNTP, deoxynucleoside 5′-triphosphate; dATP, deoxyadenosine 5′-triphosphate; dGTP, deoxyguanosine 5′-triphosphate; dCTP, deoxycytidine 5′-triphosphate; dTTP, deoxythymidine 5′-triphosphate; α^{32}P-dATP, α^{32}P-deoxyadenosine 5′-triphosphate; Hepes, *N*-[2-hydroxyethyl] piperazine-*N*′-[2-ethanesulfonic acid]; DTT, dithiothreitol; SDS, sodium dodecyl sulfate; PEG12000, poly(ethylene glycol) of 12 kDa average molecular mass; MWCO, molecular weight cut off; rpm, revolutions per minute; bps, base pairs; K_d, dissociation constant; K_a, association constant; nt(s), nucleotide(s).

identify processes within the replication fork (here leading strand-displacement DNA synthesis) that require the concerted action of two or more replication proteins as defined in a complementation assay. What we seek to elucidate are the molecular mechanisms of these manifestations of functional coupling within the T4 DNA replication fork. Additionally, our study addresses the question of the oligomeric state of gp43 DNA polymerase in the absence of other replication components. To this end, we have used sensitive analytical ultracentrifugation techniques, at physiological protein concentrations, to show first that the gp43 DNA polymerase exists as a monomer in solution at protein concentrations up to 5 μM, which is ~5 times the maximum concentration reached during cell infection (*30*). This result indicates, as in the bacteriophage T7 system (*31*), that another replication component must be responsible for the functional connection between the two T4 DNA polymerase molecules at the replication fork that is required to coordinate leading and lagging strand DNA synthesis.

We have then used these ultracentrifugation methods to look for specific physical interactions between gp43 and gp41. In the absence of NTPs, the gp41 helicase exists in a labile monomer−dimer equilibrium, this equilibrium being characterized by a monomer−dimer association constant (K_a) of $\sim 10^6$ M^{-1} (*13*). The binding of ATP or GTP drives the dimer form of gp41 into a monodisperse hexameric complex (*13*). We have been unable to detect any physical interaction between gp43 and gp41, in either its monomer−dimer or hexameric state of association, at subunit concentrations ranging up to 5 μM of each protein. This result sets the bacteriophage T4 replication system apart from those of *E. coli* (*32*−*34*) and bacteriophage T7 (*35*, *36*), since a physical interaction between helicase and DNA polymerase in the absence of DNA has been detected in both of these latter systems. The T4 replication system also differs in this regard from that of Herpes Simplex Virus type 1, where no functional interaction (and no physical interaction) between the helicase and the DNA polymerase holoenzyme has been observed (*37*). We conclude that the functional interaction of these central components of the T4 replication complex must proceed through a ternary interaction with the DNA of the replication fork. To test the hypothesis that the functional gp41−gp43 coupling is DNA-mediated, we have studied the interaction between these proteins at the replication fork.

In an earlier study, Dong et al. (*29*) used a linear primed strand-displacement DNA synthesis construct to observe a functional interaction between gp41 and gp43 that seemed to be able to catalyze the incorporation of dNTP into nascent leading strand DNA at rates as high as ~450 nts/s. However, on examining this system further, we found that the early time points used to measure the DNA synthesis rate might have contained an artifact and that while these observations are clearly qualitatively correct, the early time measurements might have been quantitatively flawed. We have therefore repeated these measurements using a rolling-circle DNA replication fork construct. In addition to remeasuring the rate of strand-displacement DNA synthesis more accurately, we have also used this approach to address another question that is fundamental to understanding the functional coupling mechanism. That is, we have asked whether specific protein−protein interactions between the homologous T4 gp41 helicase−gp43 polymerase pair are required to permit effective strand-displacement DNA synthesis within this simple model system or (especially in light of our inability to detect any specific or nonspecific interaction between gp41 and gp43 in the absence of DNA) whether heterologous DNA polymerases might also be able to form a functional replication subassembly with the T4 gp41 helicase.

We find that gp41 and gp43 can assemble onto a replication fork and form a minimal replication complex that is capable of strand-displacement DNA synthesis at a rate of ~90 nts/s in a macromolecularly crowded environment. In contrast, a functional minimal replication complex involving either gp41 and Klenow fragment or gp41 and T7DNApol could not be assembled. This result alone suggests that a specific DNA-mediated interaction (either direct or indirect) between the bacteriophage T4 proteins might be essential for strand-displacement DNA synthesis. However, we have also shown that the processive DNA polymerases (T4 gp43 DNA polymerase holoenzyme and T7DNApol.thx), tested in our assay with T4 gp41 helicase, can both perform strand-displacement DNA synthesis at a rate of ~250 nts/s. Our data show additionally that the assembly (or loading) of the helicase onto the replication fork is less efficient with the heterologous helicase-polymerase pair, revealing that the specific T4 helicase−polymerase coupling reaction may contribute primarily during the initial assembly of the replication fork. We have used these results to approach the following mechanistic questions about the helicase−polymerase coupling reaction: (i) What are the characteristics of the specific DNA-mediated gp41−gp43 coupling? (ii) How might the DNA component of the replication fork mediate the specific gp41−gp43 reaction? (iii) What are the molecular bases for the different replication rates that we observe? and (iv) Where, within the entire T4 DNA replication reaction (assembly versus elongation), is the specific (homologous) DNA-mediated helicase-polymerase coupling required?

MATERIALS AND METHODS

Reagents and Buffers. All chemicals used in these studies were of analytical reagent grade. Buffers were filtered, degassed, and temperature equilibrated before use. The nonhydrolyzable ATP analogue (ATPγS) was purchased from Boehringer Mannheim. PEG12000 was obtained from Fluka; polynucleotide kinase and the DNA molecular weight marker, MWM XV, were from Boehringer-Mannheim; deoxynucleotides and adenosine 5′-triphosphate were from Amersham Pharmacia Biotech; and γ^{32}P-adenosine 5′-triphosphate (3000 Ci/mmol) and α^{32}P -deoxyadenosine 5′-triphosphate (3000 Ci/mmol) were from NEN. Lambda DNA−*Hin*dIII digest, Klenow fragment (3′ → 5′ exo$^-$) and T7 DNA polymerase (unmodified) [which we call T7DNApol.thx] were obtained from New England Biolabs. T7DNApol (3′ → 5′ exo$^-$) was the generous gift of Dr. Smita Patel of the New Jersey Medical Center. The JM109 *E. coli* strain was obtained from Promega.

Protein Purification and Characterization. T4 gp41 helicase and gp43 DNA polymerase, gp43 exo$^-$, gp44/62, gp41, and gp45 were purified and stored as described previously (*38*−*40*). Stock solutions of both proteins were judged to be > 95% pure, based on analyses of Coomassie Blue stained

SDS−polyacrylamide gels. Protein concentrations were determined by UV absorbance at 280 nm, using molar extinction coefficients of 7.6×10^4, 1.3×10^5, 1.91×10^4, and 1.23×10^5 $M^{-1}cm^{-1}$ for monomeric gp41, monomeric gp43, monomeric gp45, and gp44/62 complex, respectively. All protein concentrations are reported in units of protein monomers.

Sample Preparation for Sedimentation Velocity Experiments. Two buffers differing in KOAc concentration were used in these studies. Both contained 33 mM Hepes, 6 mM $Mg(OAc)_2$, and 1 mM DTT, pH 7.5. SV_{medium} buffer contained 50 mM KOAc, whereas SV_{low} buffer contained 20 mM KOAc. Proteins were dialyzed against 1 L of SV_{low} or SV_{medium} buffer for 2 h at 4 °C using a Spectra/Por 16-Well microdialyzer apparatus (Spectrum) containing a Spectra/Por CE dialysis membrane with a 10 000 MWCO. The microdialyzer was connected to a pump whose flow rate was set to 7 mL/min. Samples with volumes of 30 to 60 μL were loaded into each well. After dialysis, samples were centrifuged at 12 000 rpm for 15 min at 4 °C, and the supernatants were saved. The protein concentrations of the supernatant solutions were measured using UV absorbance at 280 nm. From 85 to 100% of the input protein was recovered after dialysis. The recovered proteins were then diluted to the desired concentration with either SV_{low} or SV_{medium} buffer. When present, ATPγS was added to a final concentration of 0.35 mM.

Sedimentation Velocity Experiments. Analytical sedimentation velocity runs were performed in the Beckman Optima XL-I Analytical ultracentrifuge. Scrupulously cleaned 1.2-cm path-length double-sector ultracentrifuge cells equipped with either aluminum or Epon aluminum-filled centerpieces and quartz windows were filled with 400 and 420 μL volumes of protein and buffer, respectively, in the sample and reference sectors. The cells were then loaded into an An60Ti or an An50Ti analytical ultracentrifuge rotor. Centrifugation was not started until the experimental temperature (either 20 or 5 °C) had been reached. For velocity sedimentation experiments conducted at 5 °C, the rotor and cells were precooled at 4 °C overnight, and the cells were filled and loaded at the same temperature. The experiments were run at rotor speeds of either 50 000 or 35 000 rpm, and absorbance scans at 280 nm were collected at intervals of 2.5 to 8 min. Both the van Holde-Weischet (*41*) and the time derivative or g*(s) (*42*) methods were used for data analysis. The software for the van Holde-Weischet method and various simulations ("Finite Element Simulation" and "Model s and D from MW for Four Basic Shapes") was included in the UltraScan version 4.0 for Unix provided by Borries Demeler and downloaded from http://www.ultrascan.uthscsa.edu. Software that computes g*(s) was downloaded from the RASMB site (ftp://rasmb.bbri.org/rasmb/spin). Only data analyzed by the van Holde-Weischet method are illustrated in Figure 9 of the appendix.

Radiolabeling of Lambda DNA−HindIII Digest. A 50 μL forward kinase reaction was performed in kinase buffer (50 mM Tris-HCl, 10 mM $MgCl_2$, 0.1 mM Na_3EDTA, 5 mM DTT, 0.1 mM spermidine, pH 8.2), using 2 μg of Lambda DNA−*Hin*dIII digest as substrate, with 20 units of polynucleotide kinase, 50 pmol of ATP and 50 pmol of γ^{32}P-ATP. The kinase reactions were incubated at 37 °C for 2 h. The DNA was then ethanol-precipitated to remove unincorporated ATP and resuspended in 50 μL of formamide-dye mixture (90% deionized formamide, 0.25% xylene cyanol, and 0.25% bromophenol blue).

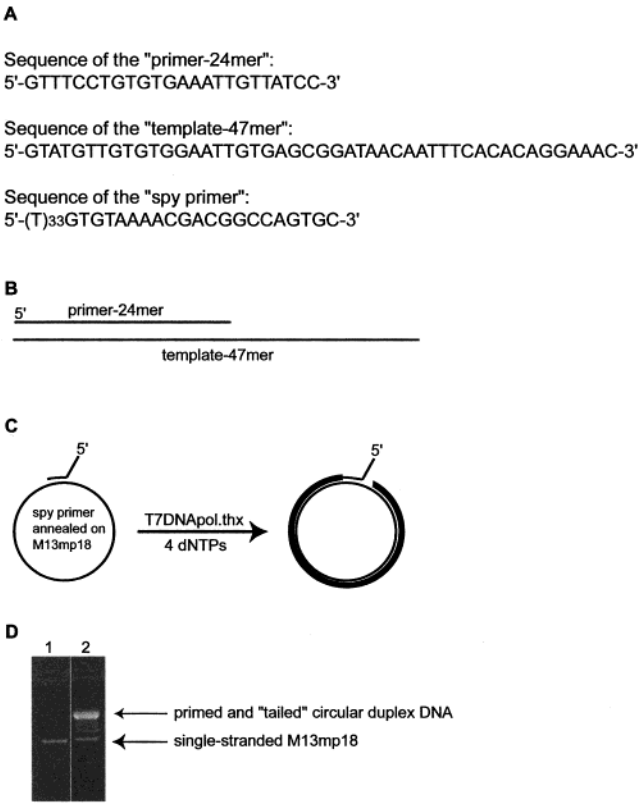

FIGURE 1: Oligonucleotides and DNA constructs. (A) Sequence of the "primer-24mer" and "template-47mer" used to prepare the primer−template junction sequence of the DNA strand-displacement synthesis construct and of the "spy primer" used to initiate synthesis of the primed and "tailed" circular duplex DNA. (B) Schematic representation of the primer−template junction formed by annealing the primer-24mer and template-47mer. (C) Outline of the procedure used to prepare the primed and tailed circular duplex DNA. The spy primer is annealed onto M13mp18 and extended after addition of T7DNApol.thx and the 4 dNTPs. The newly synthesized DNA is represented by the thicker line. Proteins were removed by a phenol−chloroform extraction followed by ethanol precipitation. (D) An ethidium bromide stained 0.8% agarose electrophoresis gel showing the circular single-stranded M13mp18 band (lane 1) and the band corresponding to the primed and tailed circular duplex DNA (lane 2). Approximately 100 ng of DNA were loaded per lane.

Oligonucleotides and DNA. All the oligonucleotides used in this study were purchased from Oligos, Etc. and purified on a 15% polyacrylamide sequencing gel before use. The sequences of the DNA oligomers used are shown in Figure 1, panel A. The "spy primer" that was used to construct the substrate for the strand-displacement DNA synthesis assay, annealed between positions 6288 and 6307 on single-stranded M13mp18 genome. Propagation of bacteriophage M13mp18 in JM109 *E. coli* cells and preparation of the bacteriophage DNA were performed as described in ref *43*.

Assembly of the Primer-Template Junction Construct and of the Primed and Tailed Circular DNA Construct. The primer−template junction construct is shown in Figure 1, panel B. Two picomoles of "primer-24mer" were radiolabeled as described in ref *44*. They were subsequently mixed with 20 pmol of unlabeled primer-24mer and 30 pmol of "template-47mer" in a buffer containing 25 mM Hepes (pH

7.5), 60 mM KOAc, 6 mM $Mg(OAc)_2$, 0.1 mM Na_3EDTA. The primer-24mer was annealed to the template-47mer by heating at 90 °C for 2 min and slow cooling with room temperature being reached in about 2 h. An aliquot was loaded on a native 12% acrylamide gel (30:0.8 acrylamide/bisacrylamide weight ratio) to check the efficiency of the hybridization, which exceeded 90%.

The procedure followed to prepare the primed and tailed circular duplex DNA construct that was used in the strand-displacement DNA synthesis reactions is illustrated in Figure 1, panel C. Fifty picomoles of spy primer were annealed with 25 pmol of M13mp18 in the T7DNApol.thx buffer [20 mM Tris-HCl (pH 7.5), 75 mM KCl, 10 mM $MgCl_2$, and 1 mM DTT] using the heating-slow cooling process described above.The primer−extension reaction used to make the primed and tailed circular duplex DNA was started by the addition of 0.25 μM (final concentrations) of each of the four dNTPs, and 20 units of T7DNApol.thx. The final concentration of the DNA construct was 100 nM. The preparative reaction was run for 2 h at 37 °C, and the proteins were then removed by phenol−chloroform extraction. The resulting DNA construct was precipitated with two volumes of ethanol-NaOAc (0.16 M) and resuspended in water. An aliquot was loaded and subjected to electrophoresis on a 0.8% agarose gel to check that at least 90% of the single-stranded M13mp18 DNA had been converted into the desired primed and tailed circular DNA duplex (Figure 1, panel D).

Primer-Elongation Synthesis Reactions. The template-directed elongation of the primer was run for 30 s at 37 °C, with the indicated amount of enzyme and in a buffer containing 25 mM Hepes (pH 7.5), 60 mM KOAc, 6 mM $Mg(OAc)_2$, 0.1 mM Na_3EDTA, 7.5% PEG12000, 1 mM DTT, and 0.125 μM of each of the four dNTPs. The final concentration of primer−template junction construct was 3 nM. When added, gp44/62 and trimeric gp45 were at 130 and 260 nM concentrations, respectively. The DNA polymerase concentration was as indicated. The reaction was stopped by adding Na_3EDTA (pH 8) to a final concentration of 25 mM. Samples were mixed with an equal volume of formamide-dye mixture (90% deionized formamide, 0.25% xylene cyanol, 0.25% bromophenol blue), boiled, and loaded onto a 20% polyacrylamide sequencing gel. After electrophoresis (2.5 h, 30 W), the gel was dried and exposed on a Phosphorimager screen (Molecular Dynamics). Quantification of reaction products was performed using the ImageQuant software obtained from Molecular Dynamics.

Strand-Displacement DNA Synthesis Assay. Strand-displacement DNA synthesis was performed at 37 °C in a buffer containing 25 mM Hepes (pH 7.5), 60 mM KOAc, 6 mM $Mg(OAc)_2$, 0.1 mM Na_3EDTA, 1 mM DTT, 7.5% PEG12000, 2 mM ATP, 250 μM dCTP, 250 μM dTTP, 250 μM dGTP, 125 μM dATP, and < 0.16 μM α^{32}P-dATP. The concentrations of primed and tailed circular duplex DNA, gp43 and gp41 (in monomer units) were 3, 30, and 180 nM, respectively. When used, gp44/62 and gp45 (in trimer units) were at concentrations of 130 and 260 nM, respectively. T7DNApol, T7DNApol.thx, and Klenow fragment were added to final concentrations of 100 nM, 50 munit/μL and 15 munit/μL, respectively. For strand-displacement DNA synthesis reaction at low dNTP concentrations, 25 μM dCTP, 25 μM dTTP, 25 μM dGTP, 12.5 μM dATP, and <0.16 μM α^{32}P-dATP were used. The primed and tailed circular duplex DNA and the DNA polymerase (plus accessory proteins where indicated) in the reaction buffer were preincubated for 1 min at 37 °C to promote the assembly of the DNA polymerase on the DNA fork. The strand-displacement DNA synthesis reaction was then started by adding the gp41 helicase. A total of 3.5 μL of the reaction mixture was quenched at various time intervals by adding 3 μL of alkaline stop buffer [15 mM Na_3EDTA (pH 8), 150 mM NaOH, 7.5% Ficoll, and 0.075% bromocresol green]. Samples were chilled on ice after quenching, and then boiled before loading on the agarose gel. DNA products were analyzed on 0.45% agarose gels in alkaline electrophoresis buffer (30 mM NaOH and 1 mM Na_3EDTA). Electrophoresis was run for 45 h at 1.5 V/cm. The alkaline gels were then soaked in TBE buffer (89 mM Tris, 89 mM boric acid, and 2 mM Na_3EDTA) for 40 min and dried for 80 min at 60 °C, and then exposed on a Phosphorimager screen (Molecular Dynamics). Quantification of reaction products was performed using the ImageQuant software (Molecular Dynamics).

RESULTS

We have used sedimentation velocity techniques to check the homogeneity of our proteins, to measure the sedimentation coefficients of gp43 polymerase and of gp41 helicase, and to analyze the sedimentation behavior of mixtures of gp41 and gp43. We also performed sedimentation velocity simulation to estimate lower limits for various equilibria. The results of these experiments are presented in the appendix.

Sedimentation Velocity Experiments Show that gp43 Polymerase Is a Monomeric Protein and That It Does Not Physically Interact with gp41 Helicase in the Absence of DNA at Physiological Protein and Salt Concentrations. The corrected sedimentation coefficient for gp43 ($S_{20,w}$) is 5.5 (± 0.1)S (see Appendix, Figure 9, panel A, and Table 2). The sedimentation properties of the polymerase are not affected by the presence of ATPγS or by changes in salt concentration and temperature (data not shown). We conclude that this value of $S_{20,w}$ corresponds to the monomeric form of gp43 and estimate that the lowest total gp43 concentration at which our data could not rule out an interaction is ~20 μM (see Appendix, Table 3). Gp41 in the presence of ATPγS is characterized by an $S_{20,w}$ of 10.4 (± 0.1)S (see Appendix, Table 2). This species corresponds to the hexameric form of the gp41 helicase. In the absence of ATP or its non-hydrolyzable analogue, ATPγS, gp41 protein at a monomer concentration of 3.3 μM sediments as a homogeneous species (data not shown), with an $S_{20,w}$ = 4.9 (± 0.1)S (see Appendix, Table 2) corresponding to the dimeric form of the helicase.

We then investigated samples containing mixtures of gp43 and gp41 at different concentrations and show that monomeric gp43 polymerase and hexameric gp41 helicase sediment independently. Indeed, all samples tested showed two independently migrating boundaries. The species present under the slower sedimenting boundary was characterized by an $S_{20,w}$ of ~5.5S, which is close to the value obtained for gp43 polymerase sedimenting alone, and the species present under the faster sedimentating boundary was characterized by an $S_{20,w}$ of ~10S, which is close to the value measured for the hexameric gp41 helicase in isolation (see Appendix, Figure 9, panel B). Furthermore, the concentra-

tion of protein present under each moving boundary matched exactly the input concentration [see Appendix, Table 4, compare OD% (measured) with OD% (expected)], indicating that no protein was lost during the course of the experiments. We also analyzed samples containing mixtures of both proteins at different concentrations, but in the absence of ATPγS, and show that monomeric gp43 and dimeric gp41 also sediment independently (see Appendix, Figure 9, panel C). Lowering the salt concentration or temperature did not reveal any physical interaction between gp41 and gp43 (data not shown). We performed sedimentation velocity simulations to confirm that dimeric or hexameric gp41 and gp43 do not physically interact and to estimate that the lower limit values for K_d for a putative complex between hexameric gp41 and gp43 or dimeric gp41 and gp43 are ~27 and ~55 μM, respectively (see Appendix, Table 3).

Determination of DNA Polymerase Concentrations for Use in the Strand-Displacement DNA Synthesis Assay. To permit direct comparison of the synthesis activity of the different DNA polymerases used in the strand-displacement DNA synthesis assay, we performed primer−extension experiments with fixed amounts of the primer−template junction construct (Figure 1, panel B) and increasing amount of the various DNA polymerases. By plotting the fraction of primer extended in a 30 s reaction (see Materials and Methods) as a function of DNA polymerase concentration (Figure 2, panels A and B), we found that concentrations of 15 munit/μL of Klenow fragment, 100 nM of T7DNApol and 50 munit/μL of T7DNApol.thx gave the same primer extension efficiency as a 30 nM concentration of T4 gp43. This suggests that the different DNA polymerases display the same total degree of binding-polymerization activity on such a template at these respective final concentrations. Therefore, we used 30 nM of gp43, 15 munit/μL of Klenow fragment, 100 nM of T7DNApol, and 50 munit/μL of T7DNApol.thx to permit direct comparison of rates in the strand-displacement DNA synthesis experiments.

Determination of the Rate and Efficiency of the Strand-Displacement DNA Synthesis Reaction. The strand-displacement DNA synthesis assay with all DNA polymerases was performed using the primed and tailed circular duplex DNA construct as template. This construct contains a single-stranded 5′-tail sequence and a primer−template junction onto which the gp41 helicase and the relevant DNA polymerase, respectively, can be loaded (for details of the DNA construct see Figure 1, panel C). In this assay, the gp41 helicase, once loaded onto the DNA, unwinds the DNA duplex and generates a single-stranded DNA template that can then be "copied" by the DNA polymerase. We characterized each strand-displacement reaction by measuring its DNA synthesis rate and efficiency.

Alkaline gel electrophoresis was used to separate the DNA product chains by size. Figure 3, panels A and B, and Figure 4, panels A and B, show that a size distribution of DNA products is obtained in these reactions, rather than a single DNA species of defined size. This follows because the reaction is not synchronized with respect to the helicase loading step. The reaction starts with the addition of gp41 to a DNA construct preloaded with DNA polymerase. Therefore, the loading of the gp41 helicase must occur prior to the start of the DNA unwinding−polymerization process. As a consequence, we have used the size of the largest DNA

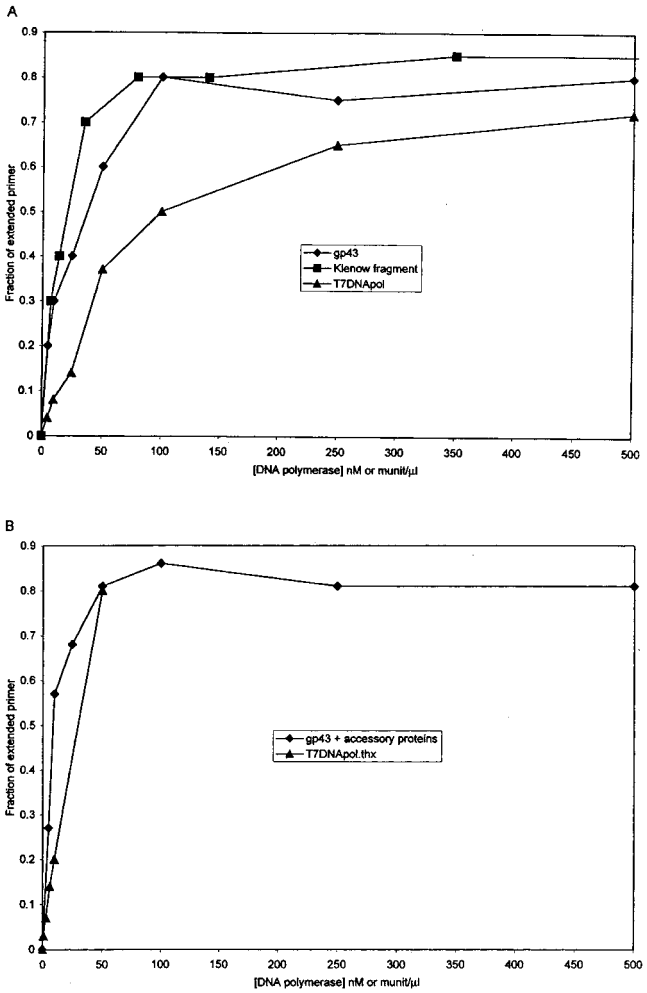

FIGURE 2: Fraction of the primers of the primer−template junction construct extended as a function of the concentrations of various DNA polymerases. (A) The primer−template junction construct (radiolabeled on the 24mer) was maintained at 3 nM within the reaction mixture, and increasing amount of nonprocessive DNA polymerases (gp43 and Klenow fragment) were added to extend the primer-24mer. Reactions were run for 30 s, after which the products were separated on a 20% polyacrylamide sequencing gel and the gel was exposed on a phosphorimager plate for data analysis. (For details see Materials and Methods.) (B) Reactions were run as in panel A, except that processive DNA polymerases (gp43 + accessory proteins and T7DNApol.thx) were used.

synthesized at each time point to measure the rate of DNA synthesis, to minimize the contribution of the time involved in helicase loading to the measured rate.

The size of the largest DNA product was determined as follows. Scanning a given lane of the gel, from the well to the bottom of the gel, generated a graph showing the radioactivity (in arbitrary units) as a function of the distance from the well (Figure 3, panel B, and Figure 4, panel B). We then determined the *x*-coordinate of the graph point whose *y*-coordinate is equal to 50% of the maximal radioactivity. Using a standard curve showing the size of DNA as a function of the distance from the well (generated with the λ-*Hin*dIII molecular weight marker), we were able to assign a size to each *x*-coordinate position. Since the reaction substrate contains ~7200 base-pairs (Figure 1, panel C), the size of the largest DNA synthesized is equal to size of the largest DNA product (in nucleotides) minus the 7200 nts originally present. We plotted the size of the largest DNA

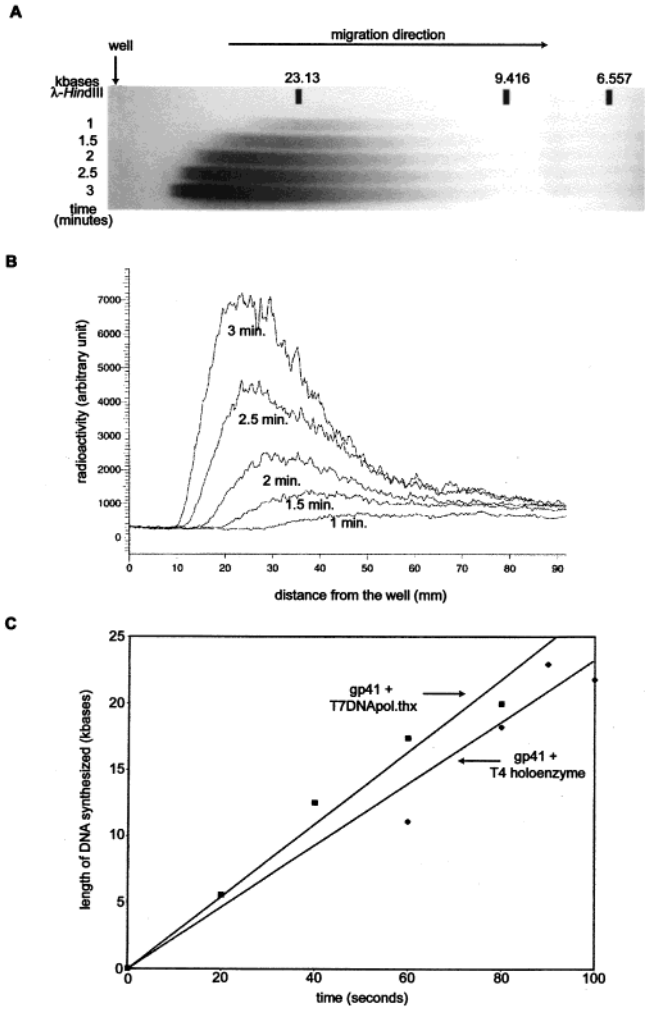

FIGURE 3: Strand-displacement DNA synthesis with processive DNA polymerases. (A) Autoradiogram of a strand-displacement DNA synthesis assay performed with the primed and tailed circular duplex DNA (3 nM), gp43 (30 nM), gp44/62 (130 nM), gp45 (260 nM trimers), and gp41 (180 nM monomers). The DNA was preincubated with the gp43 DNA polymerase holoenzyme for 1 min at 37 °C, and the reaction was started by adding the gp41 helicase. Samples were quenched at the times indicated, and then loaded onto a 0.45% agarose gel in alkaline electrophoresis buffer. After electrophoresis (45 h, 1.5 V/cm), the gel was soaked in TBE buffer, dried, and exposed on a X-ray film or on a Phosphorimager screen (Molecular Dynamics) for quantitative analysis. (B) Each scan represents the distribution of the radioactivity along one of the gel lanes shown in Figure 3, panel A. (C) The length of the newly synthesized DNA (see text for details of length determination) is plotted as a function of time to measure the rate of DNA synthesis (slope of the line). The different data points come from three different experiments, using largely nonoverlapping time points. At duplicate time points, the size of the synthesized DNA is the same within a 15% standard error. For the T7DNApol.thx reaction, this final concentration of the enzyme was 50 munit/μL.

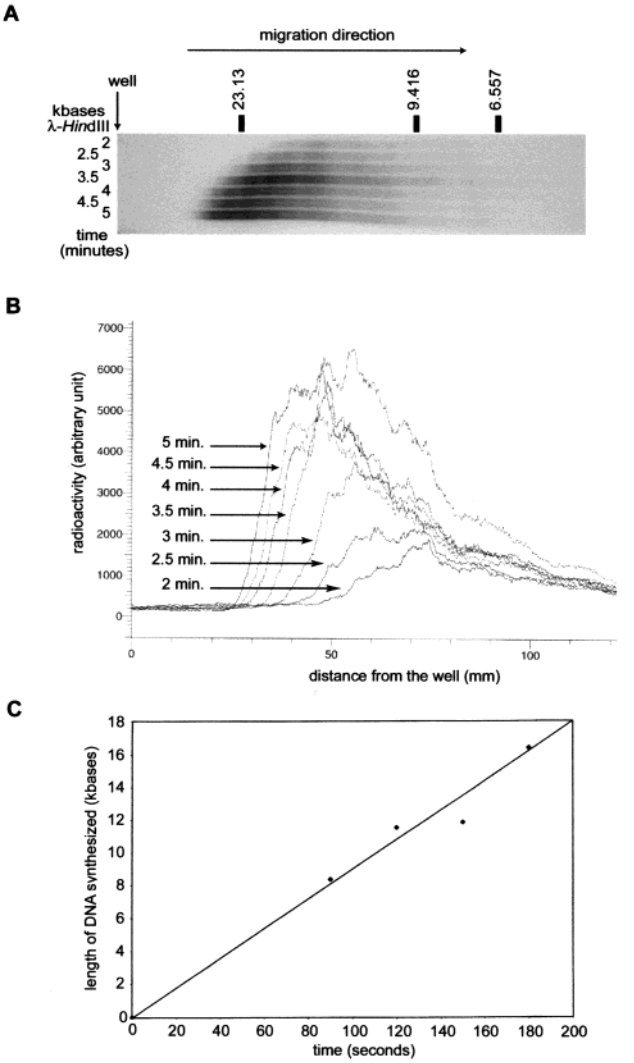

FIGURE 4: Strand-displacement DNA synthesis with the T4 gp43 polymerase and the gp41 helicase. The panels and reaction conditions correspond to those illustrated in Figure 3, except that the T4 DNA polymerase accessory proteins (gp44/62, gp45) were not included, and thus the DNA polymerase was nonprocessive.

synthesized as a function of time to determine DNA synthesis rates (Figure 3, panel C, Figure 4, panel C, and Figures 5 and 6). Since the length of synthesized DNA was equal to zero at $t = 0$, all lines in Figure 3, panel C, Figure 4, panel C, and Figures 5 and 6 were forced to go through the origin of the graph.

We note also that all DNA synthesis rates were measured within a time window corresponding to the total incorporation of less than 25 000 nts. We checked that the standard curve used to determine the product sizes was still accurate for the longer DNA fragments (around 25 000 nts) by performing experiments with the MWM XV marker (containing linear DNA fragments from 2392 to 38 412 nts). Similar results were obtained (data not shown). The time window used corresponds to the incorporation of, at most, ~2 pmol of total dNTPs per 2.5 μL of sample volume. Over this time period, the rate of DNA synthesis with all the DNA polymerases tested was constant, although beyond this point the rate of synthesis began to decrease. This observation cannot reflect depletion of the initial dNTP pool, since the total incorporation of 25 000 nts in our samples would only decrease the total concentration of free dNTPs by ~1 μM. It seems more likely that the observed decrease in synthesis rate reflects the accumulation of single-stranded DNA as the reaction proceeds, which can slow the apparent rate of extension of the replication fork construct by serving as a competitive binding "sink" for the DNA polymerase and the helicase. All strand-displacement DNA synthesis rates are summarized in Table 1.

We have also measured the efficiency of the DNA strand-displacement synthesis reaction by determining the total amounts of dAMP incorporated per 2.5 μL of sample after

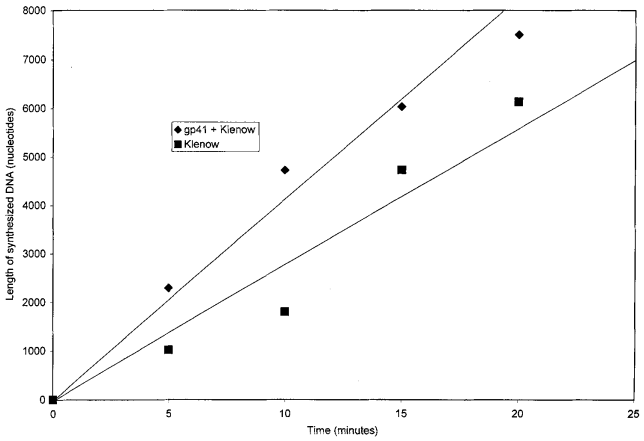

FIGURE 5: Length of the newly synthesized DNA of the extended primer of the strand-displacement DNA synthesis construct as a function of time for reactions catalyzed by the Klenow fragment of *E. coli* DNA polymerase I. Reaction conditions were as described for Figure 3. The Klenow fragment was added to a final concentration of 15 munit/μL and when present, gp41 was at a final concentration of 180 nM (in monomer units).

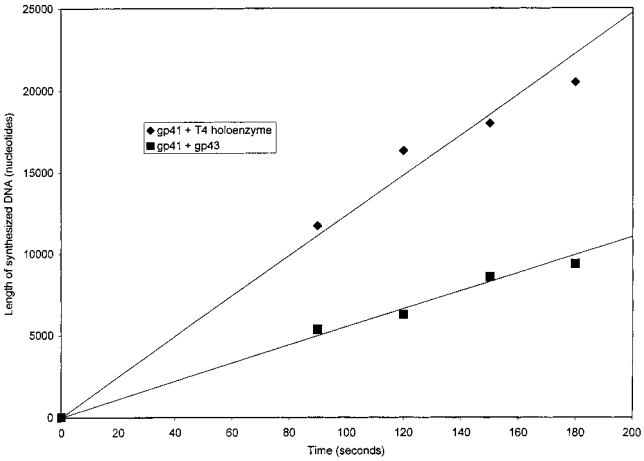

FIGURE 6: Length of the newly synthesized DNA of the extended primer of the strand-displacement DNA synthesis construct as a function of time for reactions catalyzed by the T4 DNA polymerase holoenzyme or gp43 alone in the presence of the T4 helicase at low dNTP concentrations. Reaction conditions were the same as those described for Figure 3. The primed and tailed circular duplex DNA was at a final concentration of 3 nM, gp43 was at 30 nM, and gp41 was at 180 nM (in monomer units). The final dNTP concentrations were as follows: 25 μM dCTP, 25 μM dTTP, 25 μM dGTP, 12.5 μM dATP, and < 0.16 μM α^{32}P-dATP. When present, accessory proteins were at final concentrations of 130 nM for gp44/62, and 260 nM for trimeric gp45.

the strand-displacement DNA synthesis reaction had been run for 2 min with the various helicase−polymerase pairs. These efficiencies are also summarized in Table 1. The observed differences in this parameter between helicase−polymerase pairs probably reflects different efficiencies of loading the helicase onto replication forks carrying different DNA polymerases. Indeed, the T7 DNA polymerase and the T4 DNA polymerase show similar affinities for a primer−template junction [20 nM for the T7 DNA polymerase (*45*) and 70 nM for the T4 DNA polymerase (*46*)], and at the protein concentration used, the different DNA polymerases display similar binding−polymerization activities on a primer−template junction (see above).

Strand-Displacement DNA Synthesis with Highly Processive DNA Polymerases. The DNA polymerase holoenzyme of bacteriophage T4 is highly processive (for reviews, see refs *6* and *7*). To provide a "baseline" for calibration purposes, we tested the activity of the T4 DNA polymerase holoenzyme (containing gp43, gp44/62, and gp45) in our strand-displacement DNA synthesis assay, as defined above. Control experiments showed that under the conditions of the assay, and in the absence of gp41 helicase, no strand-displacement DNA synthesis products were formed (data not shown). However strand-displacement DNA synthesis proceeded vigorously when performed in the presence of the T4 helicase, as shown in Figure 3, panels A and B. Using the calculation procedure described above, we measured a DNA synthesis rate (Figure 3, panel C) of 230 (± 30) nts/s with gp41 helicase and the T4 DNA polymerase holoenzyme system, which is very close to the rate of 250 nts/s measured previously by Cha et al. (*26*). We also measured the amount of dAMP incorporated into the nascent DNA during the strand-displacement DNA synthesis reaction, and showed that under our assay conditions, 2 (± 1) pmol of dAMP were incorporated in a 2.5 μL sample in 2 min (Table 1). This level of dAMP incorporation (i.e., the efficiency of the reaction) is similar to that reported by Spacciapoli and Nossal (*27*) in a comparable experiment performed with the T4 DNA polymerase holoenzyme, gp32, and the gp41 helicase.

Having calibrated our T4 DNA polymerase holoenzyme system against earlier published results, we then used this assay to determine whether the homologous bacteriophage T4 DNA polymerase holoenzyme is required to unwind double-stranded DNA with the T4 gp41 helicase. To approach this question, we substituted a heterologous processive DNA polymerase, the T7 DNA polymerase complexed with *E. coli* thioredoxin (T7DNApol.thx), to ask whether this processive polymerase could also work with the gp41 helicase in the strand-displacement DNA synthesis assay. Control experiments showed that under the conditions of the assay, and in the absence of gp41 helicase, no strand-displacement DNA synthesis products were formed (data not shown). As shown in Figure 3, panel C, this heterologous system synthesized DNA at the same rate [270 (± 60) nts/s] as the homologous one. However, as shown in Table 1, the efficiency of the reaction was approximately 6 times less than that of the homologous T4 system, with only 0.4 (± 0.1) pmol of dAMP being incorporated in a 2.5 μL sample after 2 min. This result suggests that while T7DNApol.thx can substitute for the bacteriophage T4 DNA polymerase holoenzyme in terms of the rate of elongation of the nascent DNA strand in the strand-displacement DNA synthesis assay, the efficiency of the assembly of the T4 helicase onto the replication fork construct is much lower in the heterologous system. Finally, we note that the macromolecular crowding agent, PEG12000, which had been shown to be essential for effective loading of the helicase in the minimal gp43−gp41 system (*29*), was not required in either of the above reactions with processive DNA polymerases, because the rates and efficiencies of strand-displacement DNA synthesis in the presence and in the absence of the macromolecular crowding agent were the same for both (data not shown).

Strand-Displacement DNA Synthesis with Nonprocessive DNA Polymerases. The T4 DNA polymerase, gp43, operating in a primer−extension assay on a single-stranded DNA template in the presence or absence of gp32, but in the absence of the T4-coded DNA polymerase accessory proteins

Table 1: Rate and Efficiency of Strand-Displacement DNA Synthesis at the Replication Fork with gp41 Helicase and Various DNA Polymerases[a]

	gp43 + accessory proteins		T7DNApol.thx			Klenow fragment of *E. coli* DNA polymerase I		gp41 + gp43 + accessory proteins (low dNTPs)	gp41 + gp43 (low dNTPs)
	−gp41	+gp41	−gp41	+gp41	gp41 + gp43	−gp41	+gp41		
DNA synthesis rate (nts/s)	0	230 (± 30)	0	270 (± 60)	90 (± 10)	5	7	125 (± 10)	55 (± 5)
reaction efficiency [b]	ND[c]	2 (± 1)	ND	0.4 ± (0.1)	0.05−0.1	ND	ND	ND	ND

[a] In all reactions, the primed and tailed circular duplex DNA was at 3 nM, gp41 (in monomer units) at 180 nM, gp44/62 at 130 nM, and gp45 (in trimer units) at 260 nM. ATP was kept at 2 mM. When not indicated, the dNTP concentration was 250 μM dCTP, 250 μM dTTP, 250 μM dGTP, 125 μM dATP, and < 0.16 μM of α^{32}P-dATP. Under low dNTPs conditions, the reaction mixture contained 25 μM of dCTP, 25 μM of dTTP, 25 μM of dGTP, 12.5 μM of dATP, and < 0.16 μM of α^{32}P-dATP. Gp43, T7DNApol, T7DNApol.thx, and Klenow fragment were added to final concentrations of 30 nM, 100 nM, 50 munit/μL, and 15 munit/μL, respectively. [b] Reaction efficiency in units of picomoles of dAMP incorporated in a 2.5 μL sample after 2 min of synthesis. [c] ND means not determined.

(gp44/62 and gp45), is effectively nonprocessive or distributive (*47*). We performed strand-displacement DNA synthesis in the absence of the accessory proteins to determine whether a processive DNA polymerase is required for our rolling-circle replication assay. Controls showed that gp43 alone cannot bring about any strand-displacement DNA synthesis under our reaction conditions (data not shown). However, strand-displacement DNA synthesis does occur with our standard DNA construct (Figure 1, panel C), at a rate of 90 (± 10) nts/s, using only the gp41 helicase and the nonprocessive gp43 DNA polymerase (Figure 4, panel C). We note that, unlike in the strand-displacement DNA synthesis assays performed with a processive DNA polymerase, this reaction requires the molecular crowding agent, PEG12000, to increase the loading efficiency of the helicase sufficiently to permit DNA synthesis, as previously reported by Dong et al. (*29*). In addition we note, in comparison to the reactions involving the processive polymerases described above, that the efficiency of the reaction with the nonprocessive polymerase is low, since here only 50 to 100 fmol of dAMP are incorporated into a 2.5 μL sample after 2 min (Table 1). Taking into account the differences in replication rates, this reaction is ~10 times less efficient than that performed with the T4 DNA polymerase holoenzyme, while the efficiency is more comparable to (although still lower than) that measured with the processive polymerase in the heterologous (T7DNApol.thx-T4 helicase) system.

To ask whether the strand-displacement DNA synthesis assay (at least at this level of rate and efficiency) can also be demonstrated with the T4 helicase and a heterologous nonprocessive DNA polymerase, we repeated the experiment with gp41 and the nonprocessive Klenow fragment of the *E. coli* DNA polymerase I. The results are presented in Figure 5, and show that, in the absence of gp41 helicase, the Klenow fragment is able to perform strand-displacement DNA synthesis only at the very slow rate of ~5 nts/s. However, as Figure 5 also shows, this rate of DNA synthesis is not significantly changed (to ~7 nts/s) by the addition gp41 helicase. We also showed that the nonprocessive T7DNApol (i.e., the T7 DNA polymerase functioning in the absence of thioredoxin) could not bring about any strand-displacement DNA synthesis in the absence of gp41. Furthermore, no strand-displacement DNA synthesis products were produced by the T7DNApol under our assay conditions in the presence of the T4 gp41 helicase (data not shown). These results suggest that, in the absence of a processivity factor, there is a specific requirement for the homologous T4-coded polymerase when the gp41 helicase unwinds the double-stranded DNA.

Strand-Displacement DNA Synthesis at Low dNTP Concentrations. We also performed strand-displacement DNA synthesis at low dNTP concentrations to determine whether slowing down the DNA polymerase might also slow the movement of the entire replication complex, or whether the helicase (in the presence of a saturating concentration of ATP) might "out-run" the DNA polymerase in the reaction under these conditions. To validate that lowering the dNTP concentrations results in a decrease in the rate of DNA synthesis, we performed strand-displacement DNA synthesis with T4 DNA polymerase holoenzyme and gp41 helicase at low dNTP concentrations. Under these conditions, the rate of DNA synthesis was 125 (± 10) nts/s (Figure 6). When strand-displacement DNA synthesis was performed with the homologous T4 DNA polymerase, but without the accessory proteins, the rate of DNA synthesis dropped to 55 (± 5) nts/s. This represents a relative decrease in the rate of DNA synthesis due to lowered dNTP concentrations of ~1.6-fold, with or without the accessory proteins (see Table 1).

The unwinding rate of gp41, in the absence of a trailing polymerase, but in the presence of gp59 protein (to facilitate helicase loading) has been estimated to be ~30 bps/s (*48*). Thus, the two DNA synthesis rates reported at low dNTPs are both higher than that of the helicase without a trailing polymerase. This finding supports the hypothesis that under such conditions the rate of double-stranded DNA unwinding by the helicase at the replication fork is controlled by the rate at which the trailing (or spying) polymerase can synthesize DNA (see Discussion).

DISCUSSION

In this study, we have asked whether the reported functional interaction between bacteriophage T4 helicase and DNA polymerase, either in the presence (*26*, *27*) or in the absence (*29*) of polymerase accessory proteins, could be explained by a direct, observable, and specific physical interaction between the gp41 helicase and the gp43 DNA polymerase. Our data demonstrate that, in the absence of DNA, gp43 exists as a monomer at physiological protein concentrations. Additionally, no physical interaction between the gp41 helicase and gp43 DNA polymerase could be detected over the range of protein concentrations used (between 1.5 and 5 μM and, by extrapolation via simulation,

up to concentrations exceeding 55 μM).

As a consequence of these results, we postulated that the DNA of the replication fork must be involved in mediating the direct or indirect helicase−polymerase interaction that is required for the functional coupling of these proteins. We then used a strand-displacement DNA synthesis assay to study the helicase−polymerase interaction at the replication fork. On the basis of such experiments, we reached the following conclusions. First, we showed that a specific DNA-mediated helicase−polymerase coupling exists between the T4-coded helicase and the polymerase (gp41−gp43) replication enzymes that allows this minimal replication system to replicate DNA at a rate of ∼90 nts/s, within an appropriate DNA replication fork construct and in the presence of a macromolecular crowding agent to drive helicase loading. Furthermore, as previously shown, in part, by others (*49*−*51*), we demonstrated that adding the gp45 processivity factor to the system improves the replication fork assembly process, obviates the need for a macromolecular crowding agent, stabilizes the replication components at the replication fork, and accelerates the rate of leading-strand DNA synthesis at the fork to approximately physiological rates. Finally, we have shown that a specific (homologous) DNA-mediated coupling between helicase and DNA polymerase is not required to permit the strand-displacement DNA synthesis reaction to proceed if a processive DNA polymerase is used to follow the helicase and to "report on" its activity. This illustrates that such functional protein−protein coupling does not necessarily require a direct physical interaction between the proteins involved.

T4 DNA Polymerase Is a Monomeric Protein at Physiological Salt and Protein Concentrations. Gp43 DNA polymerase sediments with $S_{20,w} = 5.5$ (± 0.1)S at concentrations up to 5 μM (see Appendix, Table 2). This value is close to that expected for a monomeric protein of this size and low asymmetry, in good accord with the disk shape determined by X-ray crystallography for the closely related DNA polymerase from bacteriophage RB69 (*52*). Using the simulation program, we found that an oblate (or disk shaped) ellipsoid with a molecular mass of 103 kDa and an axial ratio of 7.5 reproduces the experimentally measured $S_{20,w}$ values for gp43. From the crystal structure of the DNA polymerase from bacteriophage RB69 (*52*), we estimated an axial ratio of ∼3, which differs significantly from 7.5. This difference is probably because an oblate ellipsoid cannot appropriately represent the shape of the DNA polymerase observed crystallographically. In particular, our model does not take into account the presence of a hole in the center of the disk and that protein "fingers" protrude from the back of the polymerase (*52*).

It seems unlikely that the 5.5 S species corresponds to a dimer of gp43 with an elongated shape. First, simulation studies indicated that such a component (with a molecular mass of 206 kDa and an $S_{20,w} = 5.5$S) would have an axial ratio of 23, which is highly improbable given the known axial ratio of the monomeric DNA polymerase from bacteriophage RB69 (∼3). In addition, extensive attempts at chemical cross-linking of gp43 (data not shown and F. Dong, unpublished data) were all negative. Therefore, we believe that the 5.5S species corresponds to monomeric gp43. During cell infection, it has been estimated that gp43 is present at a concentration of ∼800 molecules/cell, corresponding to a total polymerase concentration of ∼1 μM (*30*). We have estimated the lower concentration limit at which a putative gp43 dimer might form to be ∼20 μM (see Appendix, Table 3). Therefore, our data suggest that gp43 also exists as a monomer in vivo, although macromolecular crowding in vivo might decrease this threshold limiting value (*53*).

Neither the Dimeric nor the Hexameric Form of T4 Helicase Interacts Physically with the T4 DNA Polymerase at Physiological Salt and Protein Concentrations. Since gp41 must hydrolyze ATP to translocate directionally along single-stranded DNA and to unwind double-stranded DNA, it is likely that the helicase cycles through three distinct liganded forms during translocation and unwinding. These forms correspond to a nucleotide-free, an ATP-bound and an ADP-bound, species. We considered that the ATPγS-bound form of gp41 should comprise a stable mimic of the putative ATP-bound forms of the T4 helicase. The fact that we are dealing with two noninteracting protein species (at least in the range of protein concentrations that are physiologically relevant and accessible to us experimentally) in our studies of mixtures of gp41 and gp43 in the presence of ATPγS is supported by three different kinds of observations (for details see Appendix): (i) two discrete boundaries are seen in the sedimentation velocity scans of the mixtures; (ii) the distribution plots derived from the scan analysis indicate the presence of two distinct species, one sedimentating at ∼5.5S and corresponding to a gp43 monomer and the other sedimenting at ∼10S and corresponding to a gp41 hexamer; and (iii) the proportion of each species deduced from the distribution plot matches exactly to the original input ratio of protein components. Mixtures of gp41 and gp43 in the absence of ATPγS run as a single boundary in the sedimentation velocity scans. The $S_{20,w}$ distribution plots obtained for these systems indicate that the mixed samples contain protein species with $S_{20,w}$ values ranging from 4.9 to 5.5S. Neither increasing protein concentration nor decreasing salt concentration and temperature significantly changed the values of $S_{20,w}$ obtained.

As our simulation studies showed, these behaviors can be well explained by a model involving two noninteracting proteins with $S_{20,w}$ values equal to those of gp41 and gp43. This leads us to conclude that neither the nucleotide-free nor the ATPγS-bound form of gp41 interact with gp43 DNA polymerase within the range of protein concentrations used. We were therefore able to estimate that the K_d for the formation of a putative $(gp41)_2$−gp43 and $(gp41)_6$−gp43 complex must be ≥ 55 and 27 μM, respectively, and that the favorable standard free energy of formation (ΔG°_{bind}) for such complexes at 25 °C cannot exceed ∼ −6 kcal/mol. The in vivo concentrations of gp41 and gp43 are in the range of 1.5−5 μM (*30*). If a dilute solution used in an in vitro experiment can reproduce the in vivo state, our data would suggest that no gp41−gp43 complex forms at in vivo protein concentrations. However, the cytoplasm does correspond to a "macromolecularly crowded" solution, and thus the thermodynamic activities of the protein components (i.e., their effective concentrations) may be higher in the cell (*53*).

How Can the Functional Interaction between gp43 DNA and gp41 Be Explained in the Absence of a Direct Physical Interaction between these Proteins? The absence of a direct physical interaction between gp41 and gp43, taken together with previous strand-displacement DNA synthesis assays that

have shown a strong functional interaction between the T4 helicase and polymerase in the presence (*26*, *27*) or in the absence (*29*) of the polymerase accessory proteins, suggest that the interaction of these central components of the T4 replication complex must involve the DNA of the replication fork. This conclusion, in turn, raises the following questions: Is the bacteriophage T4 DNA polymerase specifically required to achieve strand-displacement DNA synthesis with the gp41 helicase? Can a heterologous polymerase, functioning either processively or nonprocessively, work with the T4 helicase to achieve strand-displacement DNA synthesis, and if so, at what rate and with what efficiency? To answer these questions, we have used a strand-displacement DNA synthesis assay involving the T4 helicase in partnership with both processive and nonprocessive (and homologous and heterologous) DNA polymerases.

The DNA of the Replication Fork Mediates a Specific gp41−gp43 Coupling that Has Significant Functional Consequences. The T4-coded gp43 polymerase, the Klenow fragment of *E. coli* DNA polymerase I, and the T7 DNA polymerase, working in isolation, are effectively nonprocessive DNA polymerases at physiological salt concentrations. As shown previously in our laboratory (*29*), and as further elaborated here, strand-displacement DNA synthesis can be driven by the homologous two component T4 helicase−polymerase system. However, such synthesis does not occur if the homologous polymerase is replaced by either the Klenow fragment or nonprocessive T7 DNA polymerase. This suggests that a specific DNA-mediated gp41−gp43 "couple" is required during DNA synthesis that allows gp43 (but not the Klenow fragment or the T7 DNA polymerase) to be held at the primer−template junction of the replication fork while the gp41 helicase unwinds the double-stranded DNA ahead of the fork. Such a specific helicase−polymerase interaction has also been demonstrated with the bacteriophage T7 DNA replication system (*54*).

We show here that the minimal gp41−gp43 replication complex can replicate DNA at a rate of ∼90 nts/s. The assumption that gp41 and gp43 move together as a complex at the replication fork is confirmed by the results of the strand-displacement DNA synthesis assay performed at low dNTP concentrations in this study. We show in those experiments that lowering the dNTP concentrations not only slows down the gp41−gp43 DNA polymerase holoenzyme complex, but also slows down the minimal gp41−gp43 replication complex to the same (relative) extent, suggesting that the helicase unwinding rate is dependent on the synthesis rate of the trailing polymerase.

The T4 Helicase−Polymerase Couple Is Much More Processive Than the Two Proteins Working Independently. Gp41 and gp43, working separately, are poorly processive under physiological salt conditions. Thus T4 DNA polymerase, extending a hybridized primer on a single-stranded DNA template at physiological salt concentrations, can only elongate the primer by a few nts before dissociating, while the T4 helicase in isolation can only translocate along single-stranded DNA for a few hundred nts (*6*, *14*, *55*). In contrast, these proteins both gain significantly in effective processivity when they work together at a DNA fork, since nascent DNA fragments that are greater than ∼15 000 nts in length can be detected within 3 min after initiation of the unwinding−polymerization reaction in a strand-displacement DNA synthesis reaction that is effectively a single turnover process.

Indeed, we can argue that the re-assembly of a replicating fork construct after protein dissociation is unlikely for the following reason. Strand-displacement DNA synthesis generates single-stranded DNA to which gp41 can bind and along which it can, in principle, translocate in an ATP-dependent manner. We know the efficiency (50−100 fmol of dAMP incorporated after 2 min of reaction in a 2.5 μL sample) and the rate (∼90 nts/s) of the reaction (Table 1). Assuming an ∼20 nt binding site size for gp41 (*55*) and that the binding of gp41 to the single-stranded DNA that is generated by the reaction or to the ss-dsDNA junction site present at the fork are equally likely, we can calculate that ∼70% of the potential binding sites for gp41 will be located on single-stranded DNA generated by the strand-displacement DNA synthesis reaction after two minutes. This percentage will, of course, increase as the reaction proceeds further. Obviously, these new single-stranded DNA sequences will serve as traps for the gp41 and will compete with the functional gp41 binding site that is located at the fork. This makes the rebinding of gp41 to a replication fork after dissociation unlikely, meaning that these strand-displacement DNA synthesis experiments effectively represent single-turnover processes. In addition, the gain in processivity of both enzymes when working together at the fork indicates that the putative specific DNA-mediated gp41−gp43 coupling that is responsible for activity is maintained during the entire polymerization reaction along the fork construct.

The Unwinding Rate of the gp41 Helicase Is Significantly Increased by the Trailing DNA Polymerase. Raney and coworkers (*48*) have investigated the kinetics of gp41 DNA unwinding using a rapid-reaction quench-flow technique with a DNA fork that was formed by hybridizing two partially complementary oligonucleotides. The resulting fork contained two 30 nt regions of single-stranded DNA and a 30 bp duplex. Under single-turnover conditions (achieved by using a DNA trap that prevented the reformation of the substrate after unwinding) with saturating gp41 and in the presence of the T4 helicase loading protein, gp59, these workers reported that unwinding of the 30 bp duplex proceeded at a rate of ∼30 bps/s. It has been reported that gp59 is a T4-specific DNA fork binding protein (*56*) that drives loading of the hexameric gp41 onto replication forks and recombination intermediates (for a review see ref *57*), although it remains unclear whether gp59 actually translocates with the active helicase during the unwinding process. Therefore the 30 bps/s rate probably represents an upper limit for the unwinding rate of the unassisted gp41 helicase. A similar unwinding rate has been found for the *E. coli* DnaB replication helicase in the absence of DNA polymerase III holoenzyme (*32*). We note that this gp41−gp59 unwinding rate is at least 3 times slower than the replication rate catalyzed by the minimal gp41−gp43 replication couple (∼90 nts/s), meaning that the specific gp41−gp43 pair is able to drive double-stranded DNA unwinding at a significantly greater rate than can be achieved by gp41 itself, even under optimal unwinding conditions.

How Might the DNA of the Replication Fork Mediate the Specific gp41−gp43 Interaction? The possibility of assembling a minimal gp41−gp43 replication complex, and the gain in processivity of both proteins at the replication fork, might be explained by a mutual stabilization of the

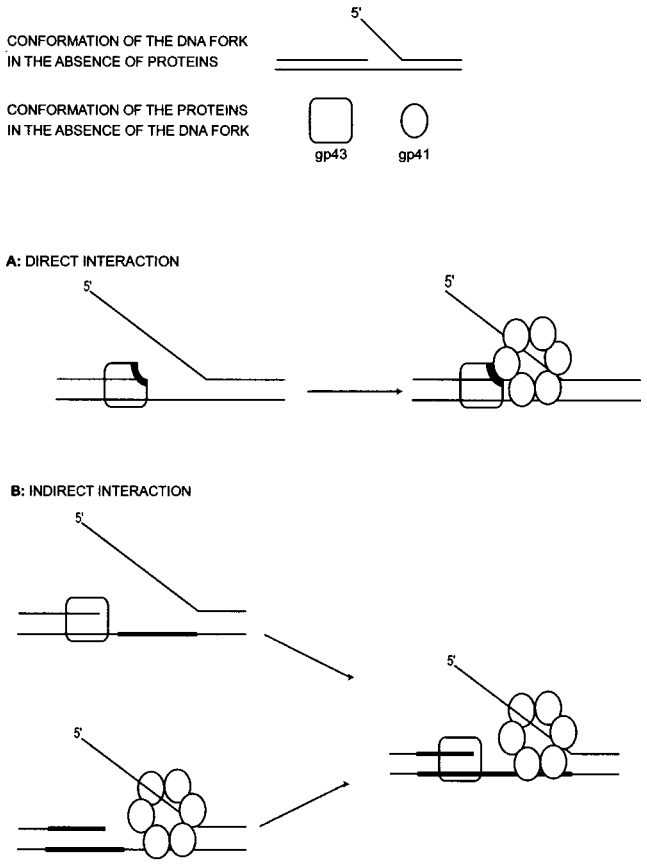

FIGURE 7: Schematic representation of the DNA mediated gp41−gp43 interaction. (A) Here the DNA mediates a direct physical interaction between gp43 and gp41 in the presence of ATP. As an example, we show a model in which gp43 adopts a new conformation upon binding to the primer−template junction. This new conformation is recognized by gp41. (B) Here the DNA mediates an indirect interaction between gp43 and gp41. In this example, there is no direct contact between the proteins, and upon binding to its substrate, the polymerase changes the DNA conformation to induce the formation of a high-affinity binding site on the fork (thicker line) for the helicase. The binding of the helicase to this high-affinity site then increases the processivity of the helicase.

proteins at their respective sites of action within the fork as a consequence of additional (and/or tighter) binding interactions. Thus the DNA fork might stabilize a direct and specific gp41−gp43 interaction, or it might mediate an indirect helicase−polymerase interaction (or coupling) as illustrated schematically in Figure 7.

In accord with the direct interaction hypothesis, it is possible that either the DNA polymerase or the helicase (or both) acquire a new conformation (or conformations) that creates a specific interaction site for complex formation between the homologous helicase and the polymerase (Figure 7, panel A). This hypothesis is not in contradiction with the results presented above, since crystal structures of variously liganded DNA polymerases have revealed that the enzyme is likely to adopt several conformations during a single nucleotide addition (polymerization) cycle (for reviews, see refs *58*−*60*), and one of these conformations could certainly be specifically recognized by the homologous helicase. It is also known that gp41 adopts a new conformation when it binds to the lagging template strand of DNA (*13*), and this conformation could be reciprocally recognized by the DNA polymerase. In addition, given that our primed and tailed duplex DNA construct, and more generally, any DNA fork, carries a DNA binding site for both the helicase and the DNA polymerase, it is likely that the gp41−gp43 direct interaction, whether it involves new protein conformations due to DNA binding, could be stabilized at the fork as a consequence of the high local concentration of both proteins at this locus. For all these reasons, the additional binding free energy provided by the fork is expected to stabilize the binding and the interactions of both proteins.

The indirect interaction (or indirect coupling) hypothesis involves no direct interactions between the helicase and the DNA polymerase at the fork. Rather, as illustrated in Figure 7, panel B, the binding of one of the proteins to its DNA site might induce the formation of a higher affinity site for the other protein elsewhere within the fork. The resulting stabilization would then increase the processivity of both proteins. To be specific, the binding of the gp43 DNA polymerase to the primer−template junction might create (or stabilize) a high-affinity site for the gp41 helicase on the lagging strand within the replication fork. Such a DNA site might comprise a "preformed fork", with single-stranded DNA exposed on both the leading and the lagging strand templates, on which the unwinding activity of gp41 helicase might be optimal (*11*). Reciprocally, a gp43 high-affinity substrate might be created by the binding of gp41 to the lagging strand at the fork.

It is also possible that the specific DNA-mediated gp41−gp43 coupling involves a combination of both direct and indirect interactions. Experiments are currently in progress to test these possibilities. Our results with the gp41-T7DNApol.thx couple suggests that this heterologous coupling is likely to be indirect, as shown in Figure 7, panel B. The fact that the DNA fork can modulate the affinity between replication proteins, and therefore mediate specific interactions, has been reported for the *E. coli* DNA replication complex, in which the DNA polymerase III holoenzyme develops a higher affinity for the β-clamp on binding to DNA, perhaps as a consequence of the induction of extra contacts between the polymerase and the DNA of the replication fork (*61*).

Possible Origins of the Observed Changes in Replication Rate as a Consequence of Helicase−Polymerase Coupling within the Replication Fork. (a) Contribution of the DNA Polymerase. An upper limit of ~30 bps/s for the rate of the DNA unwinding reaction driven by gp41 alone can be deduced from the Raney et al. study (*48*). Our results show that the minimal gp41−gp43 replication complex synthesizes DNA at a rate of ~90 nts/s, and when coupled with a processive DNA polymerase this rate can increase to ~250 nts/s. Thus gp43 alone increases the gp41 unwinding rate by a factor of 3, and a processive polymerase can increase this rate 8-fold. How might the putative (specific) DNA-mediated gp41−gp43 coupling, or the presence of a processive trailing polymerase behind the gp41 helicase, work to speed up the helicase unwinding activity?

During strand-displacement DNA synthesis, the polymerase traps the product of the helicase reaction (i.e., single-stranded DNA) as it appears, thereby preventing the separated DNA strands from reannealing. The simultaneous trapping of the reaction products of gp41 by the DNA polymerase might diminish the occurrence of helicase "slippage" (signaled by additional ATP hydrolysis not linked to translocation and DNA unwinding), such as that posited for bacte-

riophage T7 helicase (*62*). Preventing such slippage would obviously increase the observed unwinding rate of the helicase. Since a nonprocessive DNA polymerase and a processive DNA polymerase do not stimulate the gp41 unwinding rate to the same extent, we envision that they might also not diminish gp41 slippage to the same extent.

(b) Contribution of the Processivity Clamp. Our experiments with gp43 DNA polymerase in the absence or presence of the accessory proteins confirm previous studies (*47*, *63*−*67*) that have shown that the T4 gp45 processivity clamp not only renders DNA synthesis on a primed single-stranded DNA template more processive, but also significantly speeds the replication rate. In the absence or presence of the T4 DNA polymerase accessory proteins, strand-displacement DNA synthesis occurs at ∼90 and ∼230 nts/s, respectively. At the low dNTP concentrations we have used, the relative stimulation of the DNA synthesis rate by the polymerase accessory proteins is the same as at saturating concentrations of the dNTP. Thus this increase is probably a direct consequence of the increased stability of the DNA polymerase holoenzyme on its template, due to its interaction with the topologically linked (to the DNA) gp45 processivity clamp. We have also confirmed that gp45 stabilizes the replication machinery by noting that the macromolecular crowding agent, PEG12000, which is absolutely required to permit strand-displacement DNA synthesis with gp41 and gp43, can be omitted when the DNA polymerase accessory proteins are present.

(c) "Out-Running" the DNA Polymerase. Finally, we note that the rate of helicase unwinding in our strand-displacement DNA synthesis assay is controlled by the rate of synthesis of the DNA polymerase, since lowering the dNTP concentrations slows down the DNA replication machinery. However, in principle, the helicase could out-run the DNA polymerase if the speed of the DNA polymerase is low enough. This is probably what happened in the experiments in which the gp41 helicase was mixed with the Klenow fragment polymerase. Under these conditions, gp41 moves about 6 times faster than does the Klenow fragment (30 bps/s versus 5 nts/s). As a consequence, the single-stranded DNA on the leading strand exposed by the gp41 is not immediately trapped by the Klenow fragment and can reanneal with the complementary lagging strand (Figure 8). This might explain why gp41 is not capable of increasing the rate at which the Klenow fragment performs strand-displacement DNA synthesis. The gp41−Klenow fragment couple can thus be considered to exemplify the uncoordinated activity of the two enzymes.

Is the Specific DNA-Mediated gp41−gp43 (Direct or Indirect) Interaction Required Only during Replication Fork Assembly, Only during Elongation DNA Synthesis, or for Both Processes? The fact that effective strand-displacement DNA synthesis can occur with the processive T7DNApol.thx-T4gp41 couple suggests that a specific DNA-mediated gp41−gp43 functional coupling is not required for the elongation reaction if a processive DNA polymerase is used to report the activity of the helicase. We note that a similar result has been obtained with the Herpes Simplex Virus type 1 DNA replication complex (*37*). These two sets of data illustrate that coupling between the helicase and the polymerase to achieve a high elongation rate can proceed without a specific physical interaction between the proteins.

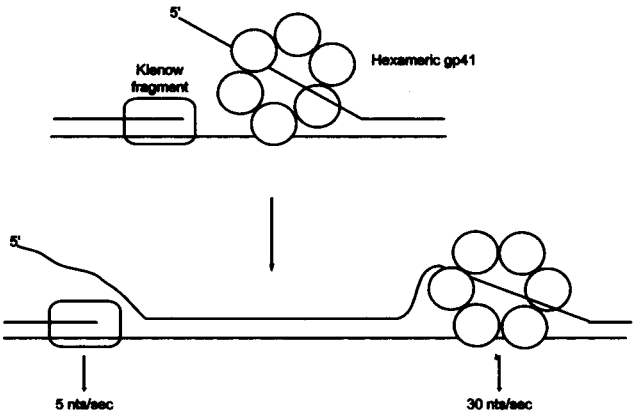

FIGURE 8: Schematic representation of a model in which the helicase "out-runs" the polymerase. Here the gp41 and the Klenow fragment of *E. coli* DNA polymerase I are shown assembled on the DNA fork prior to adding dNTPs. As the reaction proceeds, gp41 unwinds the double-stranded DNA at a rate of ∼30 bps/s, whereas Klenow fragment synthesizes the DNA at a rate of ∼5 nts/s. Since the single-stranded DNA generated by gp41 cannot be immediately trapped by the Klenow fragment, it will reanneal with its complementary strand. Therefore, the gp41 helicase in this model out-runs the Klenow fragment polymerase.

In contrast, the efficiency of strand-displacement DNA synthesis decreases ∼6-fold when T7DNApol.thx is used in place of the T4 DNA polymerase holoenzyme, suggesting that a specific DNA-mediated (direct or indirect) interactions between the homologous T4 polymerase and helicase is probably required for effective assembly (or loading) of the helicase onto the replication fork. We can thus ask whether the specific DNA-mediated gp41−gp43 coupling that is required for effective helicase loading is maintained during elongation. This question is more easily addressed with leading strand DNA replication, because here the DNA polymerase need not cycle off the DNA template. Since our results suggest that the specific DNA-mediated helicase−polymerase coupling occurs as soon as the replication fork is assembled, this coupling could also be maintained during the polymerization reaction. This notion is also supported by the observation that functional gp41−gp43 coupling is observed in the absence of the processivity factor during elongation and is also consistent with the fact that the interaction between gp43 and the processivity factor is "loose" and does not change the structure of the polymerase (*68*).

A definitive answer is more difficult to obtain for lagging strand DNA synthesis, since the lagging strand polymerase must effectively dissociate from its template after each Okazaki fragment has been synthesized. Our data show that the DNA fork mediates a direct or indirect interaction between the helicase and the DNA polymerase. Since a primer−template junction for the lagging DNA polymerase is not permanently present at the fork, it is unlikely that the functional coupling of the helicase to polymerase can be maintained. This would suggest that the helicase is probably not responsible for assembling the two T4 DNA polymerases at the replication fork, since our results show that gp43 exists as a monomer at physiological protein concentrations.

In *E. coli* (*34*) and in bacteriophage T7 (*31*, *69*), the same lagging DNA polymerase is recycled at each Okazaki fragment. This is achieved for the *E. coli* DNA polymerase III holoenzyme by two means. First, the *E. coli* DNA

polymerase holoenzyme actually contains two DNA polymerase core enzymes (for a review see ref *3*). In addition, in the *E. coli* system the direct physical helicase−polymerase interaction ensures that the leading DNA polymerase does not cycle off the DNA (*34*). Therefore, the lagging DNA polymerase of *E. coli* remains at the replication fork with the leading strand polymerase and is recycled. The situation is different for the T7 DNA polymerase, which does not dimerize by itself (*31*). It has been proposed that the T7 single-stranded DNA binding protein (gp2.5) serves to recruit and recycle the lagging DNA polymerase (*69*). If the same lagging DNA polymerase is recycled at each Okazaki fragment in the T4 system, we can speculate that the single-stranded DNA binding protein of T4 (gp32) might be comparably involved in recruiting and recycling the lagging strand DNA polymerase.

CONCLUSIONS

The results that we have reported in this paper demonstrate that the DNA of the replication fork mediates a specific functional coupling between the gp41 helicase and gp43 DNA polymerase of bacteriophage T4. This has been manifested here by the use of a DNA construct capable of efficient strand-displacement DNA synthesis. Since the T4 helicase and DNA polymerase are both poorly processive when operating independently, this finding shows that the two proteins can function cooperatively and provides a well documented example of functional protein coupling. Indeed, this protein couple, within an appropriate DNA fork context, can be viewed as a minimal DNA replication complex that is active in a macromolecular crowding environment, which, in this respect, resembles the environment of the cytoplasm of the cell (*53*, *70*).

We have hypothesized that the DNA fork can mediate either a direct or an indirect helicase−polymerase interaction (Figure 7). The efficiency of this minimal replication complex in terms of fork assembly and rate can be improved by adding the T4 polymerase accessory proteins, which increase the processivity of the DNA polymerase. We have also shown that the specific requirement for the bacteriophage T4 DNA polymerase does not apply if the DNA polymerase used as the helicase "trailer" is fully processive. This suggests that functional interaction with a trailing processive DNA polymerase is sufficient to confer processivity on the gp41 helicase and to increase its unwinding activity. This result is compatible with a protein−protein coupling reaction in the absence of a direct physical interaction. It will be interesting to see whether another type of helicase "follower" molecule that can trap the product of the helicase reaction (e.g., a single-stranded DNA binding protein) can also confer processivity onto the gp41 helicase once the loading reaction is complete. The results obtained by Roman and Kowalczykowski (*71*) using T4 gp32 or *E. coli* SSB protein as trapping agents for the RecBCD helicase (which can load onto double-stranded DNA at a blunt-end site) suggests that this is likely to be so.

If we do assume a direct physical interaction between gp41 and gp43 mediated by the DNA (as described in Figure 7, panel A), our present data do not permit us to determine whether this interaction is strong or weak. However, it may be useful to compare our gp41−gp43 coupling system with the interaction between the T4 DNA polymerase and its processivity clamp, where a loose and flexible interaction between the sliding clamp and the DNA polymerase seems to exist (*68*). It has been recently proposed that the presence of such a flexible tether between the RB69 DNA polymerase (a close relative of the T4 DNA polymerase) and the clamp allows the polymerase to make small and rapid movements on and off the 3′ terminus without complete dissociation (*68*, *72*). The problem of torsional stress generated during coordinated leading and lagging strand DNA synthesis, of bypassing DNA lesions, and of the transfer of the 3′-DNA terminus of the nascent strand from the synthesis to the editing active site might be solved if the DNA polymerase can transiently release the DNA, while retaining its general position on the template (*68*, *72*).

Hingorani and O'Donnell (*72*) have proposed that the DNA polymerase and the helicase might be tethered to one another through a flexible peptide connector located on the DNA helicase. In the crystal structure of bacteriophage T7 DNA helicase (*73*) the acidic carboxyl terminal tail of the enzyme, which is known to interact with the DNA polymerase (*35*), is poorly structured. Hingorani and O'Donnell (*72*) have suggested that this acidic carboxyl terminal tail may serve as the flexible linker. It has been shown that truncated gp41 helicase subunits generated by limited trypsin digestion, which lack the ~20 carboxyl terminal amino acid residues, are fully competent in terms of unwinding double-stranded DNA and in promoting pentamer synthesis by the gp61 primase (*40*). However, this truncated helicase is severely impaired in its ability to function in more complex reactions involving other replication proteins; i.e., in strand-displacement DNA synthesis (*40*). It will be interesting to see whether this truncated gp41 helicase is capable of reconstituting a minimal replication complex with gp43 DNA polymerase.

ACKNOWLEDGMENT

We are grateful to Steve Weitzel for assistance during protein purification, to John Gunther for his technical assistance with the Analytical Ultracentrifuge, and to Jeffrey Hansen (University of Texas Health Science center at San Antonio) and Borries Demeler (University of Texas Health Science center at San Antonio) for helping us to solve technical analytical centrifuge problems and for advice on data analysis. We are also very grateful to our laboratory colleague, Dr. Paola Pietroni, for many helpful discussions of this work and for comments on earlier drafts of the manuscript, as well as to other laboratory members. We thank Dr. Smita Patel for providing us with T7DNApol and Dr. Nancy Nossal for providing us with the gp41 overexpressing strain.

APPENDIX

In this appendix, we describe the results of sedimentation velocity experiments that show that T4 DNA polymerase exists in monomeric form and that it does not interact in solution with the homologous T4 helicase. These measurements are extended by simulation to set limits on any residual favorable free energy of interaction that might be manifested at protein concentrations that are too high to be reached by these techniques. Sedimentation velocity measurements

represent a powerful and sensitive biophysical technique to characterize the solution behavior of macromolecules (for recent reviews, see refs *74* and *75*; for a description of the technique see ref *76*). This technique can be used to check the purity of a sample, to characterize the assembly and the disassembly mechanisms of biological macromolecules, to detect conformational changes in macromolecules and macromolecular complexes, and to estimate the total mass and component stoichiometry of a macromolecular complex. In such experiments, macromolecules are free in solution and are analyzed in their native states in biologically relevant buffers. Furthermore, the results are obtained in "real" time, since scans that display protein concentration as a function of radial distance are recorded at regular intervals. As a consequence, this is probably the most artifact-free technique for the characterization of macromolecular complexes.

We summarize here the measurements that were used to characterize the homogeneity of our proteins, to measure the sedimentation coefficients of gp41 and gp43, and to analyze the sedimentation behavior of mixtures of gp41 and gp43. Two complementary procedures for data analysis were employed in these experiments: (i) the van Holde-Weischet (*41*) procedure and (ii) the time derivative (*42*) procedure. Both methods analyze the entire sedimentation boundary and can thus useful for detecting any size heterogeneity in the sample population. The van Holde-Weischet method has an additional advantage, in that it also removes the contribution of diffusion to the shape of the boundary. This advantage is important in general, since spreading of the boundary as a consequence of diffusion can mask sample heterogeneity (*41*), and was crucial in our studies because the values of $S_{20,w}$ for gp41 and gp43 in the absence of ATP are quite similar (see below). As a consequence, we have only documented the results of the van Holde-Weischet method here, but obtained effectively the same results using the time derivative method (data not shown).

T4 DNA Polymerase Exists as a Monomer in Solution. A first set of sedimentation velocity experiment was performed at 50 000 rpm and 20 °C in SV_{medium} buffer with 3 μM gp43 DNA polymerase. Under these conditions, a single boundary is seen in all scans (data not shown). Using both the van Holde-Weischet and the time derivative analysis methods, we measured $S_{20,w}$ (the sedimentation coefficient normalized to the viscosity of water at 20 °C). For gp43, $S_{20,w} = 5.5$ ($\pm$ 0.1)S (Table 2). The profile of the distribution plot of $S_{20,w}$ across the sedimentation boundary is vertical (see Figure 9, panel A), indicating that the gp43 sample is homogeneous. Increasing the concentration of gp43 to 5 μM does not change the value of $S_{20,w}$ (data not shown). Since some of our experiments were performed in SV_{medium} buffer containing ATPγS (see below), we also performed sedimentation velocity experiments at 50 000 rpm and 20 °C in SV_{medium} buffer supplemented with 0.35 mM ATPγS to show that the sedimentation properties of the polymerase are not affected by this additive (data not shown, see Table 2). Finally, since some of our gp41−gp43 mixture experiments were performed at lower temperature (5 °C) and lower salt concentrations (in SV_{low} buffer containing 20 mM KOAc instead of the 50 mM concentration of this salt present in the SV_{medium} buffer used above), we performed sedimentation velocity experiments on gp43 under these conditions. The results showed that gp43 at a concentration of 2.5 μM sediments as a homogeneous component under these conditions, yielding again a value of $S_{20,w} = 5.5$ ($\pm$ 0.1)S (data not shown, see Appendix, Table 2). We conclude that this value of $S_{20,w}$ corresponds to the monomeric form of gp43.

Table 2: Sedimentation Coefficients ($S_{20,w}$) of gp41 and gp43 in the Absence or Presence of ATPγS[a]

	gp41		gp43	
ATPγS	−	+	−	+
Dong et al. (*13*)	5.7S	12.2S		
present data				
in SV_{medium}	4.9 ($\pm$ 0.1)S	10.4 ($\pm$ 0.1)S	5.5 ($\pm$ 0.1)S	5.5 ($\pm$ 0.1)S
in SV_{low}	5 ($\pm$ 0.1)S		5.5 ($\pm$ 0.1)S	

[a] The sedimentation coefficients reported in this table correspond to samples prepared in SV_{medium} or SV_{low} buffer, in either the presence or the absence of 0.35 mM ATPγS. The samples were run in the Beckman model XL-I analytical ultracentrifuge (at 50 000 rpm and 20 °C when the sample was in SV_{medium} buffer, or at 35 000 rpm and 5 °C when the sample was in SV_{low} buffer) and the data were analyzed by the van Holde-Weischet method included in the version 4.0 for Unix of UltraScan to obtain the $S_{20,w}$ distribution plots and then sedimentation coefficients. Samples whose sedimentation coefficients are reported in Dong et al. (*13*) contained 10% glycerol and were run under similar conditions (50 000 rpm and 20 °C).

We used these data and the simulation software included within version 4.0 for Unix of the UltraScan program to estimate a lower limit value for the dissociation constant (K_d) of a putative gp43 monomer−dimer equilibrium. Sedimentation and diffusion coefficient values of $S_{20,w} = 5.5$S and $D_{20,w} = 8.1 \times 10^{-7}$ cm^2 s^{-1} were used for the monomer, and values of $S_{20,w} = 8.8$S and $D_{20,w} = 6.2 \times 10^{-7}$ cm^2 s^{-1} were used for the dimer, and 5 μM was used as the total concentration of g43. The test value of K_d was then increased until the calculated value of $S_{20,w}$ at the midpoint of the sedimentation boundary exceeded the value for pure monomer (5.5S) by ~0.4S, corresponding to an easily observable change in $S_{20,w}$ if a complex were indeed to form. This permits us to estimate that the lowest K_d for a gp43 monomer−dimer equilibrium at which our data could *not* rule out an interaction is ~20 μM (Table 3), leading to an estimated upper limit for the favorable standard free energy of association of these species (ΔG°_{bind}) at 25 °C of ~ −6.5 kcal/mol.

States of Association of gp41 in the Presence or Absence of ATPγS. A first set of sedimentation velocity experiments was performed at 50 000 rpm and 20 °C in SV_{medium} buffer supplemented with 0.35 mM ATPγS, to drive the gp41 helicase fully into the hexameric form (*13*). Under these conditions, a single boundary is seen in all the scans for the gp41 helicase (data not shown), with an $S_{20,w} = 10.4$ ($\pm$ 0.1)S (Table 2). This species corresponds to the hexameric form of the gp41 helicase. The value of $S_{20,w}$ that we have determined in this study is somewhat smaller than that (~12.2S) previously reported for the gp41 hexamer by Dong et al. (*13*). We suggest that this difference may reflect differences in experimental conditions. In particular, the samples analyzed by Dong et al. (*13*) contained ~10% glycerol, whereas our samples were glycerol-free. We note in addition that gp41 in the presence of ATPγS appears homogeneous, but shows somewhat nonideal behavior, as manifested by a curved shape (negative slope) of the $S_{20,w}$ distribution plot. At a monomer concentration of 8.5 μM, the gp41 $S_{20,w}$ at 20 and 80% of the boundary is equal to 10.4S and 9.9S, respectively. Such a distributive plot with a

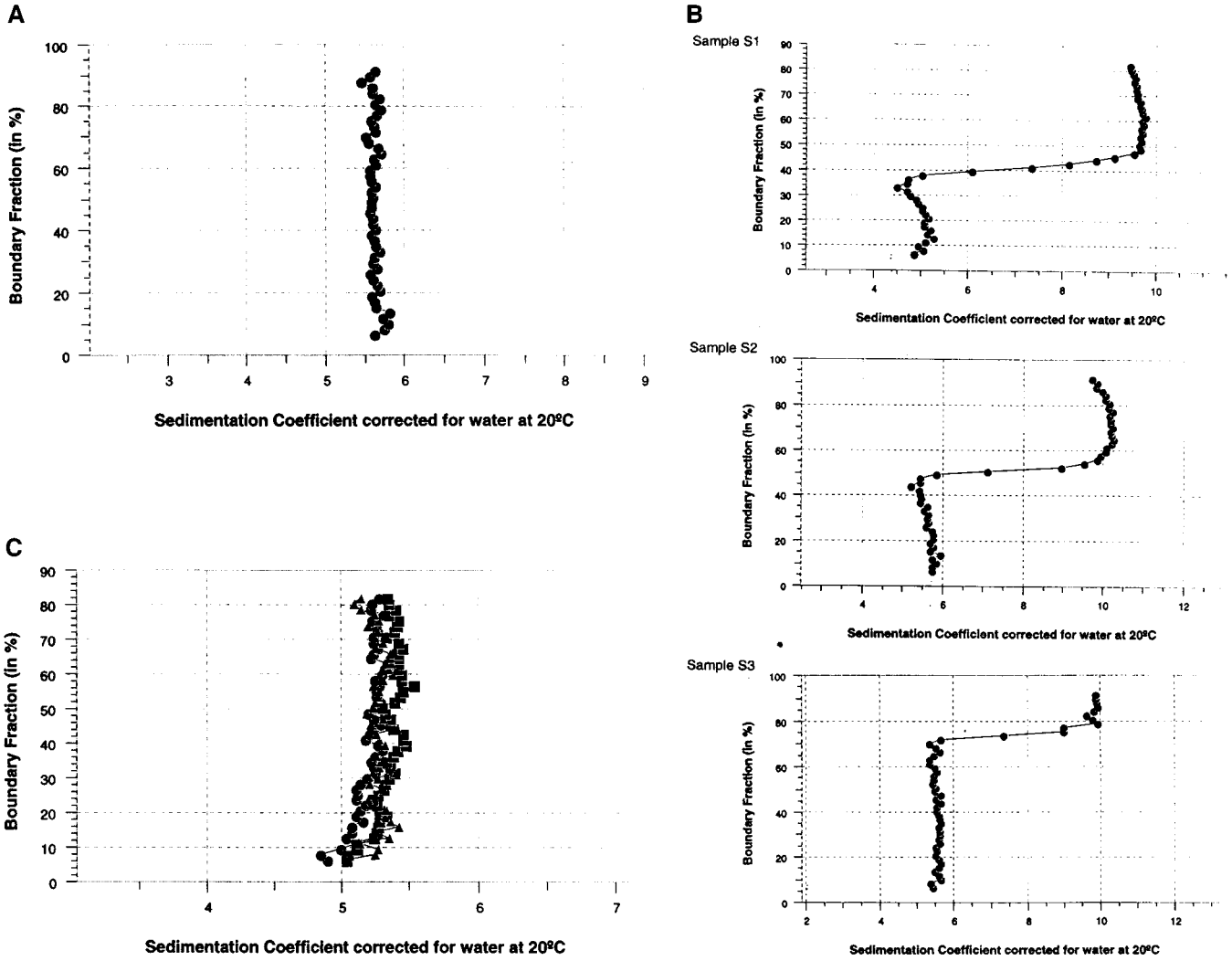

FIGURE 9: Distribution plots for sedimentation velocity runs. Samples were run and scanned in the Beckman model XL-I Analytical Ultracentrifuge at 50 000 rpm and 20 °C. Scans were analyzed by the van Holde-Weischet method to obtain the $S_{20,w}$ distribution plot. (A) A 3 μM sample of the T4 DNA polymerase (gp43) was run. (B) Sample S1, S2, and S3 were prepared in SV_{medium} buffer supplemented with 0.35 mM ATPγS to analyze the sedimentation behavior of mixtures of T4 DNA helicase hexamers and polymerase monomers. (C) Sample S1, S2, and S3 were prepared in SV_{medium} buffer to analyze the sedimentation behavior of mixtures of T4 DNA helicase monomers and polymerase monomers. (●) sample S1; (■) sample S2; (▲) sample S3.

Table 3: K_d Limits for Equilibrium Involving gp41 and/or gp43

equilibrium	K_d (μM)	maximum favorable ΔG°_{bind} (kcal/mol)
2 gp43 ⇔ $(gp43)_2$	≥ 20	−6.5
$(gp41)_2$ + gp43 ⇔ $(gp41)_2$−gp43	≥ 55	−6
$(gp41)_6$ + gp43 ⇔ $(gp41)_6$−gp43	≥ 27	−6.3

negative slope is incompatible with dissociation (in case of a dissociation, the distribution plot shows a positive slope) and often reflects the presence of significantly asymmetric or elongated macromolecules (*75*). Our final sedimentation coefficient value for the hexameric gp41 helicase, extrapolated to zero protein concentration ($S^0_{20,w}$) is to ~11S.

In the absence of ATP or its non-hydrolyzable analogue, ATPγS, gp41 helicase dissociates into a mixture of monomers and dimers (*13*). Sedimentation velocity experiments were performed in SV_{medium} buffer at 50 000 rpm and 20 °C in the absence of ATPγS to further characterize these changes. Gp41 protein at a monomer concentration of 3.3 μM sediments as a homogeneous species under these conditions (data not shown), with an $S_{20,w}$ = 4.9 (± 0.1)S (Table 2). Increasing the total gp41 concentration to 5 μM did not change $S_{20,w}$ significantly, indicating that even at the lower concentration most of the gp41 protein is in the dimer form. This result is in good accord with the K_d of ~10^{-6} M measured for this monomer−dimer gp41 equilibrium by Dong et al. (*13*). We also performed a sedimentation velocity experiment on gp41 in the absence of ATPγS at a lower temperature (5 °C) and salt concentration (SV_{low} buffer). Under these conditions, we measured an $S_{20,w}$ value of 5 (± 0.1)S (Table 2), and the sample again appeared quite homogeneous by the criterion of a vertical $S_{20,w}$ distribution profile (data not shown). This value of $S_{20,w}$ falls slightly below that previously measured for the purely dimeric protein (~5.7S) by Dong et al. (*13*). We suggest that this difference may again reflect the presence of glycerol in the samples investigated by these workers.

Monomeric gp43 Polymerase and Hexameric gp41 Helicase Sediment Independently. Having completed the above control measurements with each protein alone, we then investigated samples containing mixtures of gp43 and gp41 in SV_{medium} buffer supplemented with 0.35 mM ATPγS.

Table 4: Sedimentation Coefficients ($S_{20,w}$) of gp41 and gp43 Run as Mixtures in the Presence of ATPγS[a]

	gp41 + gp43 + ATPγS					
	sample S1		sample S2		sample S3	
	slow species	fast species	slow species	fast species	slow species	fast species
$S_{20,w}$	~5S	~9.5S	~5.5S	~10S	~5.5S	~10S
OD% (measured)	~35	~65	~50	~50	~70	~30
OD% (expected)	~30	~70	~50	~50	~70	~30

[a] Samples were prepared in SV_{medium} buffer supplemented with 0.35 mM ATPγS and run in the Beckman model XL-I analytical ultracentrifuge in SV_{medium} buffer at 50 000 rpm and 20 °C. Data were analyzed by the van Holde-Weischet method included in the version 4.0 for Unix of UltraScan to obtain the distribution plot and subsequently the sedimentation coefficients and proportion of each protein in terms of OD_{280} [OD% (measured)]. The OD% (expected) is the contribution in terms of OD_{280} of the slow and the fast species that is expected from the total initial input.

Samples were prepared at various protein concentration ratios and subjected to sedimentation velocity analysis to look for interactions between the helicase and the polymerase. The centrifugation conditions used were 50 000 rpm and 20 °C, and three different (molar) protein input ratios were studied. Sample S1 contained 5 μM gp41 and 1.5 μM gp43, sample S2 contained 3 μM gp41 and 1.5 μM gp43, and sample S3 contained 3 μM gp41 and 4 μM gp43. In these samples (S1, S2, and S3), gp43 contributed 30, 50, and 70% of the total OD_{280}, respectively. The total protein optical density (OD_{280}) did not exceed unity in any of the experiments.

Two discrete boundaries were observed in all three sets of scans for these "mixture" experiments (data not shown). Our data analysis procedures permit us to measure the $S_{20,w}$ of the macromolecular species responsible for each boundary and also to estimate the concentration of protein present under each boundary. The calculated results are shown in Figure 9, panel B, and are summarized in Table 4. In all three samples, there was no sign of any component faster sedimenting than the hexameric helicase in any of these three samples, and no protein was lost during sedimentation. These data show that the hexameric gp41 helicase and the gp43 polymerase do not interact to form a complex at any concentration of the protein components below 5 μM.

Monomeric gp43 and Dimeric gp41 also Sediment Independently. Samples containing mixtures of both proteins at different concentrations, but in the absence of ATPγS, were also analyzed. A first series of experiments was performed in SV_{medium} buffer at 50 000 rpm and 20 °C. Sample S1 contained 2 μM gp41 and 1.6 μM gp43, sample S2 contained 4 μM gp41 and 3.2 μM gp43, and sample S3 contained 5 μM gp41 and 5 μM of gp43. For all three samples, a single boundary was observed in the sedimentation velocity scans (data not shown). Data analysis revealed some heterogeneity in these three samples, indicating the presence of protein species with values of $S_{20,w}$ ranging from 4.9 to 5.5S in all the samples, showing that the sedimentation coefficients for all the boundaries in the mixed systems run between the values measured above for the two proteins run separately (Figure 9, panel C). This result suggests the absence of any equilibrium involving larger species.

To examine this issue further, and assuming that low salt concentration and low temperature might favor any latent interactions that might be present, we also performed a second set of sedimentation velocity experiments on these mixtures at lower temperature (5 °C) and in SV_{low} buffer. We examined the sedimentation behavior of two mixtures containing both proteins at two different total concentrations under these low temperature−low salt concentration conditions. Sample S1 contained 2 μM gp41 and 2 μM gp43 and sample S2 contained 4 μM concentrations of each protein. In both mixtures, a single boundary was seen in the scans, and the distribution plots yield an average $S_{20,w}$ value of ~5.25S (data not shown) for both runs, with no observable separation into two components. Again, the observed value of $S_{20,w}$ for the boundary corresponding to the mixture falls between the values expected for gp41 and gp43 run separately. Furthermore, increasing the concentration of protein by a factor of 2 does not change the shape or the position of the distribution plot. This suggests that even under these presumably favorable (for interaction) conditions of salt, protein concentration, and temperature, gp41 and gp43 still do not associate to any measurable extent.

Using the simulation software included in the UltraScan program, we performed sedimentation velocity simulations for a system of two noninteracting species. We used values of $S_{20,w}$ of 4.9S and 5.5S and values of $D_{20,w}$ of 7.9×10^{-7} cm^2 s^{-1} and 8.1×10^{-7} cm^2 s^{-1}, respectively, for the two species (monomeric gp43 and dimeric gp41). We showed that separation of such a mixture into two resolvable components is not expected under these conditions, and that the position of the distribution plot along the $S_{20,w}$ axis does not change with increasing total protein concentration. Further simulations showed that either single or multiple boundary(ies) might be seen with an interacting system, depending on the stoichiometry of the complex, the K_d of the equilibrium, and the relative concentrations of each protein. More importantly, the position of the distribution plot would be shifted to higher $S_{20,w}$ values with increasing protein concentrations. Our results show a single boundary for all our mixture samples and that increasing the total protein concentration by factors of two to three does not significantly change the position of the distribution plot on the $S_{20,w}$ axis (Figure 9, panel C). These results also strongly support the conclusion that we are dealing with a noninteracting system, at least in the concentration range over which our experiments were performed.

The simulation program was also used to estimate a lower limit value for K_d for a putative complex between dimeric gp41 and gp43. Since gp41 dimers and gp43 monomers are characterized by very similar values of $S_{20,w}$ we approximated (for purposes of the simulation) the mixture of gp41 and gp43 by a single ("monomer") species with an $S_{20,w} = 5.3$S and a $D_{20,w} = 8 \times 10^{-7}$ cm^2 s^{-1}. We then estimated the hydrodynamic parameters that would correspond to a hypothetical 1:1 complex of these species ("dimer") as $S_{20,w} =$ 8.6S, and $D_{20,w} = 6.5 \times 10^{-7}$ cm^2 s^{-1}. We used 10 μM as the total concentration of potentially interacting gp41 and g43 species, since in our mixture experiments the highest protein concentrations of each species were ~5 μM. We then inserted increasing test values of K_d for complex formation until the theoretically calculated value of $S_{20,w}$ at the midpoint of the boundary for the mixture exceeded the value for pure

"monomer" (5.3S) by ~0.4S, again corresponding to an easily observable change in $S_{20,w}$ if a complex were indeed to form. This permits us to estimate that the lowest K_d for a $(gp41)_2-gp43$ equilibrium at which our data could not rule out an interaction to be ~55 μM (Table 3), providing an estimated upper limit for the favorable standard free energy of association of these species (ΔG°_{bind}) at 25 °C of ~ −6 kcal/mol (Table 3). On the basis of these $S_{20,w}$ values for the "monomer" and "dimer" species we then determined that an 0.4S increase in the $S_{20,w}$ value at the midpoint of the boundary would be observed if 12% of the total protein were "dimer", resulting in a lower limit estimate of K_d of ~27 μM, and of ΔG°_{bind} of ~ −6.3 kcal/mol for a putative complex between hexameric gp41 and gp43 (Table 3).

REFERENCES

1. von Hippel, P. H. (1998) *Science 281*, 660−5.
2. Kuriyan, J., and O'Donnell, M. (1993) *J. Mol. Biol. 234*, 915−25.
3. Kelman, Z., and O'Donnell, M. (1995) *Annu. Rev. Biochem. 64*, 171−200.
4. Baker, T. A., and Bell, S. P. (1998) *Cell 92*, 295−305.
5. Hingorani, M. M., and O'Donnell, M. (1998) *Curr. Biol. 8*, R83−6.
6. Young, M. C., Reddy, M. K., and von Hippel, P. H. (1992) *Biochemistry 31*, 8675−90.
7. Nossal, N. G. (1992) *FASEB J. 6*, 871−8.
8. Alley, S. C., Shier, V. K., Abel-Santos, E., Sexton, D. J., Soumillion, P., and Benkovic, S. J. (1999) *Biochemistry 38*, 7696−709.
9. Sexton, D. J., Berdis, A. J., and Benkovic, S. J. (1997) *Curr. Opin. Chem. Biol. 1*, 316−22.
10. Venkatesan, M., Silver, L. L., and Nossal, N. G. (1982) *J. Biol. Chem. 257*, 12426−34.
11. Richardson, R. W., and Nossal, N. G. (1989) *J. Biol. Chem. 264*, 4725−31.
12. Liu, C. C., and Alberts, B. M. (1981) *J. Biol. Chem. 256*, 2813−20.
13. Dong, F., Gogol, E. P., and von Hippel, P. H. (1995) *J. Biol. Chem. 270*, 7462−73.
14. Young, M. C., Schultz, D. E., Ring, D., and von Hippel, P. H. (1994) *J. Mol. Biol. 235*, 1447−58.
15. Yu, X., Hingorani, M. M., Patel, S. S., and Egelman, E. H. (1996) *Nat. Struct. Biol. 3*, 740−3.
16. Liu, C. C., and Alberts, B. M. (1980) *Proc. Natl. Acad. Sci. U.S.A. 77*, 5698−702.
17. Liu, C. C., and Alberts, B. M. (1981) *J. Biol. Chem. 256*, 2821−9.
18. Cha, T. A., and Alberts, B. M. (1986) *J. Biol. Chem. 261*, 7001−10.
19. Hinton, D. M., and Nossal, N. G. (1987) *J. Biol. Chem. 262*, 10873−8.
20. Nossal, N. G., and Hinton, D. M. (1987) *J. Biol. Chem. 262*, 10879−85.
21. Dong, F., and von Hippel, P. H. (1996) *J. Biol. Chem. 271*, 19625−31.
22. Jing, D. H., Dong, F., Latham, G. J., and von Hippel, P. H. (1999) *J. Biol. Chem. 274*, 27287−98.
23. Kowalczykowski, S. C., Lonberg, N., Newport, J. W., and von Hippel, P. H. (1981) *J. Mol. Biol. 145*, 75−104.
24. Huberman, J. A., Kornberg, A., and Alberts, B. M. (1971) *J. Mol. Biol. 62*, 39−52.
25. Cha, T. A., and Alberts, B. M. (1990) *Biochemistry 29*, 1791−8.
26. Cha, T. A., and Alberts, B. M. (1989) *J. Biol. Chem. 264*, 12220−5.
27. Spacciapoli, P., and Nossal, N. G. (1994) *J. Biol. Chem. 269*, 447−55.
28. Schrock, R. D., and Alberts, B. (1996) *J. Biol. Chem. 271*, 16678−82.
29. Dong, F., Weitzel, S. E., and von Hippel, P. H. (1996) *Proc. Natl. Acad. Sci. U.S.A. 93*, 14456−61.
30. Burke, R. L., Munn, M., Barry, J., and Alberts, B. M. (1985) *J. Biol. Chem. 260*, 1711−22.
31. Debyser, Z., Tabor, S., and Richardson, C. C. (1994) *Cell 77*, 157−66.
32. Kim, S., Dallmann, H. G., McHenry, C. S., and Marians, K. J. (1996) *Cell 84*, 643−50.
33. Kim, S., Dallmann, H. G., McHenry, C. S., and Marians, K. J. (1996) *J. Biol. Chem. 271*, 21406−12.
34. Yuzhakov, A., Turner, J., and O'Donnell, M. (1996) *Cell 86*, 877−86.
35. Notarnicola, S. M., Mulcahy, H. L., Lee, J., and Richardson, C. C. (1997) *J. Biol. Chem. 272*, 18425−33.
36. Guo, S., Tabor, S., and Richardson, C. C. (1999) *J. Biol. Chem. 274*, 30303−9.
37. Falkenberg, M., Elias, P., and Lehman, I. R. (1998) *J. Biol. Chem. 273*, 32154−7.
38. Morris, C. F., Hama-Inaba, H., Mace, D., Sinha, N. K., and Alberts, B. (1979) *J. Biol. Chem. 254*, 6787−96.
39. Hinton, D. M., Silver, L. L., and Nossal, N. G. (1985) *J. Biol. Chem. 260*, 12851−7.
40. Richardson, R. W., and Nossal, N. G. (1989) *J. Biol. Chem. 264*, 4732−9.
41. van Holde, K. E., and Weischet, W. O. (1978) *Biopolymers 17*, 1387−1403.
42. Stafford, W. F., 3rd. (1994) *Methods Enzymol. 240*, 478−501.
43. Maniatis, T., Fritsch, E. F., and Sambrook, J. (1989) in *Molecular Cloning: A Laboratory Handbook*, Book 1, Chapter 4, pp 4.21−4.32.
44. Maniatis, T., Fritsch, E. F., and Sambrook, J. (1989) in *Molecular Cloning: A Laboratory Handbook*, Book 1, Chapter 5, pp 5.68−5.71.
45. Patel, S. S., Wong, I., and Johnson, K. A. (1991) *Biochemistry 30*, 511−25.
46. Capson, T. L., Peliska, J. A., Kaboord, B. F., Frey, M. W., Lively, C., Dahlberg, M., and Benkovic, S. J. (1992) *Biochemistry 31*, 10984−94.
47. Newport, J. W. (1980) Ph.D. thesis, University of Oregon
48. Raney, K. D., Carver, T. E., and Benkovic, S. J. (1996) *J. Biol. Chem. 271*, 14074−81.
49. Kaboord, B. F., and Benkovic, S. J. (1993) *Proc. Natl. Acad. Sci. U.S.A. 90*, 10881−5.
50. Jarvis, T. C., Newport, J. W., and von Hippel, P. H. (1991) *J. Biol. Chem. 266*, 1830−40.
51. Reddy, M. K., Weitzel, S. E., and von Hippel, P. H. (1993) *Proc. Natl. Acad. Sci. U.S.A. 90*, 3211−5.
52. Wang, J., Sattar, A. K., Wang, C. C., Karam, J. D., Konigsberg, W. H., and Steitz, T. A. (1997) *Cell 89*, 1087−99.
53. Record, M. T., Jr., Courtenay, E. S., Cayley, S., and Guttman, H. J. (1998) *Trends Biochem. Sci. 23*, 190−4.
54. Lechner, R. L., and Richardson, C. C. (1983) *J. Biol. Chem. 258*, 11185−96.
55. Young, M. C., Kuhl, S. B., and von Hippel, P. H. (1994) *J. Mol. Biol. 235*, 1436−46.
56. Mueser, T. C., Jones, C. E., Nossal, N. G., and Hyde, C. C. (2000) *J. Mol. Biol. 296*, 597−612.
57. Nossal, N. G. (1994) *Molecular Biology of Bacteriophage T4* (Karam, J. D. Ed.) pp 43−53, American Society for Microbiology, Washington, DC.
58. Kunkel, T. A., and Wilson, S. H. (1998) *Nat. Struct. Biol. 5*, 95−9.
59. Jager, J., and Pata, J. D. (1999) *Curr. Opin. Struct. Biol. 9*, 21−8.
60. Brautigam, C. A., and Steitz, T. A. (1998) *Curr. Opin. Struct. Biol. 8*, 54−63.
61. Naktinis, V., Turner, J., and O'Donnell, M. (1996) *Cell 84*, 137−45.
62. Washington, M. T., Rosenberg, A. H., Griffin, K., Studier, F. W., and Patel, S. S. (1996) *J. Biol. Chem. 271*, 26825−34.
63. Newport, J., Kowalczykowski, S., Lonberg, N., Paul, L., and von Hippel, P. (1980) *ICN-UCLA Symp.* 485−506.
64. Mace, D. C. (1975) Ph.D. thesis, Princeton University.

65. Mace, D. C., and Alberts, B. M. (1984) *J. Mol. Biol. 177*, 279−93.
66. Mace, D. C., and Alberts, B. M. (1984) *J. Mol. Biol. 177*, 313−27.
67. Piperno, J. R., and Alberts, B. M. (1978) *J. Biol. Chem. 253*, 5174−9.
68. Shamoo, Y., and Steitz, T. A. (1999) *Cell 99*, 155−66.
69. Lee, J., Chastain, P. D., 2nd, Kusakabe, T., Griffith, J. D., and Richardson, C. C. (1998) *Mol. Cell 1*, 1001−10.
70. Cayley, S., Lewis, B. A., Guttman, H. J., and Record, M. T., Jr. (1991) *J. Mol. Biol. 222*, 281−300.
71. Roman, L. J., and Kowalczykowski, S. C. (1989) *Biochemistry 28*, 2863−73.
72. Hingorani, M. M., and O'Donnell, M. (2000) *Curr. Biol. 10*, R25−9.
73. Sawaya, M. R., Guo, S., Tabor, S., Richardson, C. C., and Ellenberger, T. (1999) *Cell 99*, 167−77.
74. Cole, J. L., and Hansen, J. C. (1999) *J. Biomolec. Tech. 10*, 163−176.
75. Demeler, B., Saber, H., and Hansen, J. C. (1997) *Biophys. J. 72*, 397−407.
76. Cantor, C. R., and Schimmel, P. R. (1980) in *Biophysical Chemistry* (W. H. Freeman and Company) Chapter 11, pp 591−642, New York.

BI001306L